Electronic Supplementary Information (ESI)

Efficient Integration of Carbon Dioxide Reduction and 5 Hydroxymethylfurfural Oxidation at High Current Density

Roger Lin*, Haoyan Yang*, Hanyu Zheng*, Mahdi Salehi, Amirhossein Farzi, Poojan Patel, Xiao Wang, Jiaxun Guo, Kefang Liu, Zhengyuan Gao, Xiaojia Li, Ali Seifitokaldani+

Materials and Chemicals

We utilized a custom-made flow cell (Figure 2) to run the experiments. Soft tubing and peristaltic pumps were ordered from Cole-Parmer. The Ag/AgCl reference electrodes and Pt plate were obtained from Corrtest Instruments Co. Anion exchange membrane Fumasep® FAA-3-PK-75, and nickel foam were bought from Fuel Cell Store. Carbon felt (Y03G028) was ordered from Alfa Aesar. KOH and NaOH pellets (85%), NaCl salt (99%), HMF (99%), FDCA (97%), Ag/AgCl in 3 M KCl solution, were purchased from Sigma Aldrich. HMFCA (98%) was bought from Cayman Chemicals; 2,5-Diformylfuran (DFF) (98%) and 5-Formyl-2-furancarboxylic acid (FFCA) (98%) were bought from TCI America. $NaH_2PO_2 \cdot H_2O$, methanol (99%), ethanol (99%), 1-propanol (99%), sulfuric acid (5.00 N) and ammonium formate (99%) were ordered from Fisher Scientific. $Ni(NO_3)_2 \cdot 6H_2O$ (99%) was purchased from Acros Organics. High-purity CO_2 (99.995%) was purchased from Linde. BJD and NexDep physical vapour deposition systems were used to produce metal vapours deposited onto electrically conductive materials as a thin metal coating under vacuum conditions. All reagent chemicals were commercially available and of analytical grade. RO water was obtained from an in-house purification system (typically 18.2 MΩ cm resistivity).

A peristaltic pump was used together with the flow cell to ensures the HMF-containing anolyte passes through the porous carbon felt electrocatalyst. When the OER was studied without biomass upgrading, the anode chamber was filled with only KOH electrolyte without HMF. Two identical Ag/AgCl reference electrodes were used, one in cathode and one in anode. Each was used to measure the potential of the half-cell it was inside. This allowed the applied potential on counter electrode to be measured during electrochemical tests.

Flow Cell Design and Importance of GDL

Cathodic carbon dioxide reduction is performed in a flow cell to enhance mass transfer and reduce CO_2 uptake in the alkaline solution. Gas diffusion layer plays a critical role in achieving higher partial current density towards the production of final products [1-3]. This phenomenon is mainly attributed to three important factors in the reaction: the CO_2 molecule diffusion path, the CO_2 source, and CO_2 uptake in bulk electrolyte [3-5]. By incorporating a gas diffusion layer (as depicted in (Figure S1), the reactant CO_2 can be more effectively transported to the catalyst surface due to a considerably reduced diffusion path (10 nm ~ 10 µm) [6]. Additionally, by delivering CO_2 in its gaseous form at higher concentration, the mass transfer limitation associated with its dissolved form in a typical H-type cell can be circumvented [1, 7]. Finally, the CO_2 dissolved in catholyte leads to carbonate/bicarbonate formation in alkaline conditions, which reduces the CO_2 availability and creates a salting issue at the cathode surface [4]. By using a flow cell electrolyzer, the performance of CO_2RR remains competitive with the HER, even at current densities higher than 50 mA/cm^2.

Electrocatalyst Synthesis

NiP catalyst

To prepare the NiP sample, 2 nm of Ni was first deposited onto a carbon felt by physical vapour deposition on both sides. To deposit NiP, a solution of 0.1 M of $Ni(NO_3)_2$ and 0.5 M of NaH_2PO_2 was prepared by dissolving 2.9374 g of $Ni(NO_3)_2$ and 5.3530 g of NaH_2PO_2 in 100 mL of RO water in an undivided cell. Linear sweep voltammogram from -0.3 V to -1.0 V (vs Ag/AgCl) was then performed for 50 cycles to the Ni-deposited carbon felt, with Pt as the counter electrode, similar to our previous work [8]. A typical NiP potentio-dynamic deposition is shown in Figure S2.

Ag and Cu catalysts

The Ag/CP, Cu/CP, Ag/PTFE (BJD), and Cu/PTFE (NexDep) catalyst samples used in this experiment were prepared via the Physical Vapor Deposition (PVD) technique using pure metal targets (99.9999% purity). With this technique, a thin layer of particles was evenly deposited at 1-2 Å/s onto the supporting material surface by sputtering the metal vapours under vacuum (10^6 torrs) using the BJD electron-beam sputter machine (Angstrom Engineering) [9]. Specifically, 200 nm of metal (Cu or Ag) was sputtered onto carbon paper at once on BJD, and 400 nm samples were sputtered onto PTFE. The 400 nm Ag sample was sputtered on BJD in two identical steps (each with 200 nm thickness) with a ten-minute break at vacuum to cool down the chamber. The 400 nm Cu preparation on NexDep included four repeats of 100 nm deposition layers, and the sample was kept in vacuum in between. Ag and Cu targets were of a purity equal to 99.99% and 99.9999% respectively, and both machines work at 7.4 kV. Specifically, Ag was sputtered with a current of 78 mA and Cu with a current close to 240 mA.

Sn catalyst

400 µL of Nafion, 100 mg of Sn nanoparticle and 20 mL of ethanol were mixed to prepare the drop cast solution. The solution was then sonicated for 15 minutes to ensure Sn nanoparticles were mixed evenly. 1 mL of the solution was dropped on 4 cm^2 of carbon paper, resulting in 1.25 mg of Sn nanoparticle and 5 µL of Nafion loaded per cm^2 area. To facilitate the evaporation of ethanol, the drop-casting was done on a hotplate set to 85 °C in a fume hood.

NiOOH catalyst

A nickel foam of dimension 2 cm × 2 cm was submerged in 2 M NaOH solution. A galvanostatic cycling was applied where an anodic current of 0.4 A was passed for 15 seconds and a cathodic current of -0.4 A for 5 seconds. This was repeated for 30 cycles, followed by a final polarization step, where an anodic current of 0.4 A was applied for 300 seconds. After the treatment, a uniform black coating (NiOOH) on the nickel foam was formed, with a supposedly thickness of more than 100 monolayers. This NiOOH electrode serves as a benchmark for the HMFOR experiments.

NiOOH layer was also formed on the NiP catalyst by applying anodic potential. The as-prepared NiP@Ni/CF became oxidized after cyclic voltammetry (CV) and was therefore named NiOOH/NiP@Ni/CF under anodic potentials. Thereafter, the catalyst is referred to NiP in this work.

Characterization

Ultra-high-resolution field emission SEM (Hitachi, Cold FE SU-8000 SEM) at 30 kV voltage was used to examine the morphology of the catalyst surface. Subsequently, EDX was used to investigate the elemental composition of the catalysts. NiP catalyst, Ni/CF and CF substrate were examined by Bruker D8 Advance powder X-ray diffractometer (XRD) with Cu Kα source for crystal structure analysis. The as-prepared and post-experiment electrocatalysts were inspected by XPS (Thermo-Scientific, K-Alpha XPS apparatus) with an Al Kα source to indicate the oxidation state and bonding present on the catalyst surface.

X-ray adsorption spectroscopy (XAS) was run at the Canadian Light Source. Soft X-ray Microcharacterization Beamline (SXRMB) was used to identify the atomic environment and oxidation states of Ni species on the catalyst. Calibration was done with Ni foam and Ni (II) oxide as standard reference samples.

Electrochemical Measurement

Electrochemical tests were carried out with potentiostats (Metrohm, PGSTAT204). Electrochemical impedance of the system was measured by the potentiostat with frequency response analysis. Ohmic loss was calculated by multiplying the system resistance (Rs) by the applied current. Applied voltage was iR corrected by subtracting the ohmic loss from the measured voltage at the electrode:

$$V_{applied} = V_{measured} - iR_s$$

Product Analysis

A Thermo Ultimate 3000 HPLC was used for liquid product detection and quantification, with a Thermo Acclaim 300 C18 column for the HMFOR tests and a Phenomenex Rezex ROA column for the CO_2RR tests. Ammonium formate (5 mM) and methanol at a volumetric ratio of 9:1 were used as the mobile phase for HMFOR samples, while 0.005 N sulfuric acid was used as mobile phase for CO_2RR samples. For liquid product examination from HMFOR tests, 1 ml of liquid sample was added to 9 ml of RO water and then further diluted with 40 ml of 0.1 M KOH to have a dilution ratio of 1:50. It was filtered using a syringe filter and filled in a 2 ml vial, then placed in the HPLC autosampler. For CO_2RR liquid product analysis, 5 ml of catholyte was sampled and 3 ml of 1 M H_2SO_4 was added to acidify the alkaline catholyte to pH ~2. The mixture was sonicated for 10-15 mins to remove dissolved CO_2 gas and filtered into a 2 ml vial for HPLC injection. UV-vis spectroscopy was used to identify and quantify formate, acetate (AA) as well as HMFOR intermediates and products; refractive index (RI) detector was used to identify and quantify alcohols. A typical HPLC chromatogram of HMFOR products are shown in Figure S19.

Gas products were analyzed and quantified using an Agilent GC 6890 (GC) with two columns using argon as the carrier gas. An Agilent HP PLOT-Q column (column 1) and an Agilent HP-PLOT MoleSieve composed of zeolite (column 2) were used. An adjustable restrictor valve was in place to direct the gas flow from column 1. At the beginning of the method, gases traveled through column 1 and were trapped in column 2. At 5.2 minutes runtime, the GC shuts column 2 with the restrictor valve to capture the faster gases, also allowing the slower gases to bypass the second column and go straight to the thermal conductivity detector (TCD). At 11 minutes runtime, the valve switched back to the initial position and gases in the column 2 were analyzed. 1 mL of gas product was sampled from the cathode gas chamber outlet using a Hamilton syringe and was manually injected into the GC.

Gas products were also analyzed and quantified using GC-FID with a methanizer for CO and ethylene. The gas outlet of the flow cell was directly connected to the GC instrument via a copper tubing and gas tight connectors. During the GC process, the instrument automatically sampled from the gas tubing (1 mL) to generate a gas chromatograph.

The gas analysis employed a Clarus 590 GC with dual columns, utilizing argon as the carrier gas. Column 1 was a HayeSep N column, and column 2 was a MoleSieve 13X. A modifiable restrictor valve directed gas flow between the columns. Initially, gases traveled through column 1, followed by trapping in column 2. At 1.20 minutes into the runtime, the GC shut column 2 with the restrictor valve, capturing faster gases. Slower gases bypassed column 2 and reached the thermal conductivity detector (TCD). At 5.05 minutes, the valve reverted, and gases in column 2 were analyzed. Post-TCD detection, gases were mixed with H_2 and entered the methanizer, where C-based gases were converted to methane before proceeding to the Flame ionization detector (FID). A typical GC chromatogram of CO_2RR products is shown in Figure S22.

TEA calculations

Mass balance calculations:

1) CO_2RR-OER System:

Basis:

Base case, 100 t/day KCOOH (potassium formate) production.

CO_2RR reaction assumptions:

30% CO_2 consumption in electrolyte to form bicarbonate, 1% loss in product separation, 10% FE to CO, 10% FE to H_2, 80% FE to KCOOH, no volume change in electrolyte.

CO_2RR separation assumptions:

98% anolyte recycled, 18.33 wt% potassium bicarbonate solubility at 20 °C,[10] 76.82 wt% potassium formate solubility at 18 °C[11].

CO_2RR calculations:

Yield of CO_2RR products in cathode:

$$Y_i = \frac{\Delta N_i}{-\Delta N_{CO_2}} = \frac{\frac{FE_i}{n_i}}{\sum_i \nu_{i,CO_2}\left(\frac{FE_i}{n_i}\right)} \times single\ pass\ conversion$$

Where N_i is the number of moles of cathode product i generated from CO_2 (CO, KCOOH) (note: number of moles of H_2 from CO_2 is 0), ν_{i,CO_2} is the ratio of stoichiometric coefficient of CO_2 to product i in CO_2RR, FE_i is Faradaic efficiency of each cathode product i, n_i is number of moles of electron per mole of product i formed.

Theoretical CO_2 required for 100 t KCOOH production = $\frac{M_{KCOOH}}{MW_{KCOOH}} \times \frac{MW_{CO_2}}{Y_{KCOOH}} = 117{,}689\,\frac{kg}{day}$

Actual CO_2 consumed for 100 t KCOOH production = $Theoretical\ CO_2\ required \div 99\% = 118{,}878\,\frac{kg}{day}$

CO_2RR products in cathode:

$$M_i = \frac{CO_2\ consumed}{MW_{CO_2}} \times Y_i \times MW_i$$

Where M_i is each cathode product generated, MW_i is the molecular weight of product i.

Potassium bicarbonate produced $= \frac{CO_2\ consumed}{MW_{CO_2}} \times 30\% \times MW_{KHCO_3} = 81{,}146\,\frac{kg}{day}$

Current required:

$$I = \sum_i \left(M_i \times \frac{n_i}{MW_i}\right) \times \frac{F}{\sum_i FE_i} = 3{,}352{,}367\ \mathrm{A}$$

Where, F is Faradaic number 96485 C/mol.

Hydrogen produced in cathode:

$$M_{cathode,H_2} = \frac{I}{F} \times \frac{MW_{H_2}}{n_{H_2}} \times FE_{H_2} = 300\,\frac{kg}{day}$$

Where MW_i is the molecular weight of product i.

Area of electrode required:

$$A_{electrode} = \frac{I}{J} = 3{,}352\ m^2$$

Where J is the current density at 0.1 A/cm^2.

Power required:

$$P_{cell} = I \times V = 7.4\ MW$$

Where V is the cell voltage at 2.2 V.

Oxygen generated in anode:

$$M_{O_2} = \frac{I}{n_{O_2}F} \times MW_{O_2} = 24{,}016\,\frac{kg}{day}$$

Where MW is the molecular weight, n_{O2} is number of moles of electron per mole of oxygen formed.

Water generated in anode:

$$M_{anode,H_2O} = \frac{M_{O_2}}{MW_{O_2}} \times n_{O_2,H_2O} \times MW_{H_2O} = 27{,}018\,\frac{kg}{day}$$

Where $n_{O2,H2O}$ is number of moles of water per mole of oxygen formed.

Water required in cathode:

$$M_{cathode,H_2O} = \sum_k \left(\frac{M_k}{MW_k} \times N_{k,H_2O} \times MW_{H_2O}\right) = 29{,}719\,\frac{kg}{day}$$

Where $N_{k,H2O}$ is number of moles of water per mole of cathode product k formed (H_2, CO, KCOOH).

Net water required in cathode:

$$M_{net\ cathode,H_2O} = M_{cathode,H_2O} - M_{anode,H_2O} = 2{,}702\,\frac{kg}{day}$$

KOH in anolyte $= M_{net,H_2O} \times C_{KOH} \times \frac{MW_{KOH}}{\rho_{H_2O}} = 151\,\frac{kg}{day}$

Where C_{KOH} is at 1 mol/L, and ρ_{H2O} is the density of water at 1.0 kg/L.

Net KOH required in catholyte:

$$M_{net,cathode,KOH} = \sum_n \left(\nu_{n,OH^-} \times \frac{M_n}{MW_n} \times N_{n,OH^-} \times MW_{KOH}\right) = 112{,}634\,\frac{kg}{day}$$

Where $N_{n,OH-}$ is number of moles of OH^- per mole of cathode and anode product n formed (H_2, CO, KCOOH, O2, KHCO3), $\nu_{n,OH-}$ is the ratio of stoichiometric coefficient of OH^- to cathode and anode product n.

Water supplied to cathode:

$$M_{cathode\ supply,H_2O} = \frac{M_{cathode,KOH}}{MW_{KOH}} \times \frac{\rho_{H_2O}}{C_{KOH}} = 2{,}011{,}316\,\frac{kg}{day}$$

Where C_{KOH} is at 1 mol/L, and ρ_{H2O} is 1.0 kg/L.

Total water required $= M_{net\ cathode,H_2O} + M_{cathode\ supply,H_2O} = 2{,}014{,}018\,\frac{kg}{day}$

Total electrolyte required $= M_{net,cathode,KOH} + KOH\ in\ anolyte \times (1 - 98\%) = 112{,}637\,\frac{kg}{day}$

Potassium bicarbonate produced:

$$M_{cathode,KHCO_3} = \frac{CO_2\ consumed}{MW_{CO_2}} \times 30\% \times MW_{KHCO_3} = 81{,}146\,\frac{kg}{day}$$

Flow to crystallizer:

$$Q = M_{cathode\ supply,H2O} + KCOOH\ produced = 2{,}112{,}326\,\frac{kg}{day}$$

Potassium formate concentration in electrolyzer outlet:

$$x_{KCOOH} = \frac{KCOOH\ produced}{Q} = 4.78\ wt\%$$

Potassium bicarbonate removed $= M_{cathode,KHCO_3} - \frac{KCOOH\ produced}{KCOOH\ solubility} \times KHCO_3\ solubility = 57{,}048\,\frac{kg}{day}$

2) HMFOR-HER System:

Basis:

Base case, 100 t/day FDCA production.

HMFOR reaction assumptions:

100% HMF conversion, 1% HMF loss in reaction, 15wt% HMF in anode inlet, 90% FE to FDCA, 5% FE to HMFCA, 5% FE to FFCA.

HMFOR calculations:

Theoretical HMF required for 100 t FDCA production (80% yield) = $\frac{M_{FDCA}}{MW_{FDCA}} \times MW_{HMF} \div 80\% = 100{,}989\,\frac{kg}{day}$

Actual HMF consumed for 100 t FDCA production = $Theoretical\ HMF\ required \div 99\% = 102{,}010\,\frac{kg}{day}$

HMFOR products in anode:

$$M_j = \frac{Theoretical\ HMF\ required}{MW_{HMF}} \times Y_j \times MW_j$$

Where M_j is each anode product j generated (FDCA, FFCA, HMFCA), Y_j is the yield of product j, MW_j is the molecular weight of product j.

Current required:

$$I = M_j \times \sum_j \left(\frac{n_j}{MW_j} \times Y_j\right) 96{,}485\,\frac{C}{mol} = 4{,}769{,}484\text{ A}$$

Where n_j is number of moles of electron per mole of product j formed, Y_j is the yield of product j, MW_j is the molecular weight of product j.

Area of electrode required:

$$A_{electrode} = \frac{I}{J} = 4{,}769\ m^2$$

Where J is the current density at 0.1 A/cm^2.

Power required:

$$P_{cell} = I \times V = 9.5\ MW$$

Where V is the cell voltage at 2 V.

Anolyte input $= Actual\ HMF\ consumed\ \times \frac{w_{anolyte}}{w_{HMF}} = 578{,}054\,\frac{kg}{day}$

KOH in anolyte $= Anolyte\ input\ \times C_{KOH} \times \frac{MW_{KOH}}{\rho_{KOH}} = 30{,}830\,\frac{kg}{day}$

Where C_{KOH} is at 1 mol/L, and ρ_{KOH} is the density of 1M KOH at 1.05 kg/L[12].

Water in anode $= Anolyte\ input - KOH\ in\ anolyte = 547,225\,\frac{kg}{day}$

Water generated in HMFOR:

$$M_{anode,H_2O} = \sum_j \left(\frac{M_j}{MW_j} \times N_{j,H_2O} \times MW_{H_2O}\right) = 50{,}931\,\frac{kg}{day}$$

Where N_{j,H_2O} is number of moles of water per mole of product j formed.

Hydrogen produced in HER at cathode $= \frac{I}{n_{H_2}F} \times MW_{H_2} = 4{,}271\,\frac{kg}{day}$

Net water required for HER at cathode $= \frac{H_2\ produced}{MW_{H_2}} \times N_{H_2,H_2O} \times MW_{H_2O} - M_{anode,H_2O} = 25{,}946\,\frac{kg}{day}$

KOH in catholyte $= \frac{KOH\ in\ anolyte}{Water\ in\ anode} \times Net\ water\ required\ for\ HER = 1{,}462\,\frac{kg}{day}$

Sulfuric acid required for adjustment to pH2 $= \frac{KOH\ in\ anolyte \times MW_{acid}}{2 \times MW_{KOH}} + \frac{10^{-pH} \times MW_{acid}}{2} \times Q_{H_2O} = 27{,}249\,\frac{kg}{day}$

Where Q_{H_2O} is the volume of the water in neutralized anolyte, assuming density of 1 kg/L.

Potassium sulfate formed $= \frac{KOH\ in\ anolyte}{MW_{KOH}} \times N_{KOH,K_2SO_4} \times MW_{K_2SO_4} = 47{,}967\,\frac{kg}{day}$

3) Combined HMFOR-CO_2RR System:

Basis:

Base case, 100 t/day KCOOH production.

CO_2RR reaction assumptions:

Same as in CO_2RR-OER system.

CO_2RR separation assumptions:

No anolyte recycled. Same solubilities of potassium bicarbonate and potassium formate as in CO_2RR-OER system.

HMFOR reaction assumptions:

Same as in HMFOR-HER system.

HMFOR-CO_2RR calculations:

Same calculations on CO_2RR half-cell regarding the CO_2RR products, net water and KOH required in cathode, electrode area and potassium bicarbonate produced and removed.

Power required:

$$P_{cell} = I \times V = 6.7\ MW$$

Where V is the cell voltage at 2 V.

HMFOR products in anode:

$$M_j = \frac{I}{F} \times \frac{MW_j}{n_j} \times FE_j$$

Where M_j is each anode product (FDCA, FFCA, HMFCA) generated, n_j is number of moles of electron per mole of product j formed, MW_j is the molecular weight of product j.

Theoretical HMF needed for FDCA, HMFCA and FFCA production:

$$M_{HMF} = \sum_m \left(\frac{M_m}{MW_m} \times MW_{HMF}\right) = 70{,}983\,\frac{kg}{day}$$

Where m is each anode product (FDCA, HMFCA, FFCA), MW is the molecular weight.

Actual HMF needed = $70{,}983\,\frac{kg}{day} \div 99\% = 71{,}700\,\frac{kg}{day}$

Assuming 15 wt% HMF is supplied with the 0.01 M KOH electrolyte.

Electrolyte flow rate = $Actual\ HMF\ consumed \times \frac{w_{anolyte}}{w_{HMF}} = 406{,}302\,\frac{kg}{day}$

KOH in anolyte $= Anolyte\ input\ \times C_{KOH} \times \frac{MW_{KOH}}{\rho_{KOH}} = 21{,}669\,\frac{kg}{day}$

Where C_{KOH} is at 1 mol/L, and ρ_{KOH} is the density of 1M KOH at 1.05 kg/L.

Water supplied to anode:

$$M_{anode\ supplied,H_2O} = M_{anode,analyte} - M_{anode,H_2O} = 384{,}632\,\frac{kg}{day}$$

Water generated in HMFOR:

$$M_{anode,H_2O} = \sum_j \left(\frac{M_j}{MW_j} \times N_{j,H_2O} \times MW_{H_2O}\right) = 35{,}798\,\frac{kg}{day}$$

Total water required in cathode:

Total water required $= M_{cathode\ supplied,H_2O} + M_{anode\ supplied,H_2O} = 2{,}395{,}949\,\frac{kg}{day}$

Total electrolyte required $= M_{cathode,KOH} + KOH\ in\ anolyte = 134{,}303\,\frac{kg}{day}$

Sulfuric acid required for adjustment to pH2 $= \frac{KOH\ in\ anolyte \times MW_{acid}}{2\times MW_{KOH}} + \frac{10^{-pH}\times MW_{acid}}{2} \times Q_{H_2O} = 19{,}153\,\frac{kg}{day}$

Where Q_{H_2O} is the volume of the water in neutralized anolyte, assuming density of 1 kg/L.

Potassium sulfate formed $= \frac{KOH\ in\ anolyte}{MW_{KOH}} \times N_{KOH,K_2SO_4} \times MW_{K_2SO_4} = 33{,}715\,\frac{kg}{day}$

Capital Cost analysis:

Costs assumptions:

FDCA selling price 1,773 $/ton.

35% balance of plant including 15% electric, 5% piping, 5% instrumentations, 10% others.

5% engineering and supervision cost and 6% construction and contractor's fee on direct costs.

10% contingency on direct and indirect costs excluding legal expense.

1% legal expense and 8% startup expense on fixed capital investment.

5% working capital on total capital investment.

CAPEX calculation using the base case for the combined HMFOR-CO_2RR system as an example:

Electrolyzer cost $= A_{electrode} \times \frac{\$460}{m^2} = \$1{,}542{,}000$

Separation capital cost

$= neutralization\ reactor\ + FDCA\ crystallizer\ +\ FDCA\ filter + bicarbonate\ crystallizer + bicarbonate\ filter$

$= \$242{,}000 +\ \$1{,}222{,}000\ +\ \$311{,}000\ +\ \$4{,}260{,}000 + \$277{,}000 = \$6{,}312{,}000$

Balance of plant $= (electrolyzer\ cost + separation\ cost) \times \frac{35\%}{1-35\%} = \$4{,}229{,}077$

Total direct costs $= electrolyzer\ cost + separation\ cost + balance\ of\ plant = \$12{,}083{,}077$

Engineering and supervision cost $= total\ direct\ costs \times\ 5\% = \$604{,}154$

Construction and contractor's fee $= total\ direct\ costs \times\ 6\% = \$724{,}985$

Contingency

$= (total\ direct\ costs + engineering\ and\ supervision\ cost + construction\ and\ contractor's\ fee) \times 10\% =\ \$1{,}341{,}222$

Legal expense

$= \frac{total\ direct\ costs + engineering\ and\ supervision\ cost + construction\ and\ contractor's\ fee}{1-1\%-10\%} \times 1\% =\ \$150{,}699$

Total indirect costs

$= engineering\ and\ supervision\ cost\ +\ construction\ and\ contractor's\ fee\ +\ legal\ expense = \$1{,}479{,}838$

Fixed capital investment $= total\ direct\ costs\ +\ total\ indirect\ costs\ = \$14{,}904{,}136$

Startup expense $= fixed\ capital\ investment \times 8\% = \$1{,}192{,}331$

Working capital $= \frac{fixed\ capital\ investment\ +\ startup\ expense}{1-5\%} \times 5\% =\ \$847{,}182$

Total capital investment

$= fixed\ capital\ investment\ +\ cstartup\ expense\ +\ working\ capital = \$16{,}943{,}649$

Operating Cost analysis:

OPEX assumptions:

90% operating factor (329 days/year).

98% anolyte KOH recycle in the OER, 100% cathode KOH recycle in the HER.

2.5% annual maintenance cost, 10% labor cost, and 10% operating supplies on the fixed capital investment.

OPEX calculation using the base case for the combined HMFOR-CO_2RR system as an example:

HMF cost $= HMF\ required \times HMF\ price = \$76{,}719/day$

CO_2 cost $= CO_2\ required \times CO_2\ price = \$5{,}148/day$

Water cost $=\ water\ required \times water\ price\ =\ \ \$7{,}188/day$

Electrolyte cost $= (net\ KOH\ required\ in\ cathode + KOH\ in\ anode) \times KOH\ price\ = \$178{,}479/day$

H_2SO_4 cost $= H_2SO_4\ required \times H_2SO_4\ price = \$4{,}980/day$

Electricity cost $=\ power\ required \times electricity\ price = \$4{,}827/day$

Maintenance cost $= fixed\ capital\ investment \times 2.5\% = \$1{,}134/day$

Labor $= fixed\ capital\ investment \times 10\% = \$4{,}537/day$

Operating supplies $= fixed\ capital\ investment \times 10\% = \$4{,}537/day$

Subtotal Operating costs $= reagent + utilities + maintenance + labor + supplies = \$287{,}559/day$

Plant overhead $= \frac{Subtotal\ operating\ costs}{1-5\%-2\%} \times 5\% =\ \$15{,}460/\text{day}$

Administrative cost $= \frac{Subtotal\ operating\ costs}{1-5\%-2\%} \times 2\% =\ \$6{,}184/\text{day}$

Total operating costs $= subtotal\ operating\ costs + plant\ overhead + admin\ cost = \$309{,}204/day$

Yearly profit $= (Product\ income - total\ operating\ cost) \times\ operating\ factor = -\$1{,}665{,}346/year$

Calculation of Net Present Value

NPV Assumptions:

38.9% income tax.

10% nominal interest rate.

10-year MACRS for depreciation.

20% salvage value of fixed capital investment and all working capital recovered at the end of 20-year period.

NPV calculation using the base case for the combined HMFOR-CO_2RR system as an example:

In year zero, the facility is built, hence the cumulative present value:

$Year\ 0\ cumulative\ value\ =\ -fixed\ capital\ investment\ -\ (working\ capital\ +\ startup\ expense) = -\$16{,}943{,}649$

$Year\ 1\ depreciation\ = 10\%\ fixed\ capital\ investment\ =\ \$1{,}490{,}414$

$Year\ 1\ net\ earnings = (yearly\ profit - depreciation) \times (1 - income\ tax)^{*} = -\$2{,}656{,}583$

*Note: income tax is only applicable to positive yearly revenue.

$Year\ 1\ cash\ flow = Year\ 1\ net\ earnings + Year\ 1\ depriciation = -\$3{,}155{,}760 + \$1{,}490{,}414 = -\$1{,}665{,}346$

$Year\ 1\ discounted\ cash\ flow = \frac{Year\ 1\ cash\ flow}{(1 + interest\ rate)^{year}} = \$1{,}513{,}951$

$Year\ 1\ cumulative\ present\ value = Year\ 0\ cumulative\ value + Year\ 1\ discounted\ cash\ flow = -\$18{,}457{,}600$

Same calculations for year 2 to year 20 except for the depreciation, which follows 10-year MACRS.

$Year\ 20\ additional\ income = 20\%\ fixed\ capital\ investment + working\ capital = \$3{,}828{,}010$

$Year\ 20\ cash\ flow = Year\ 20\ net\ earnings + Year\ 20\ depriciation + Year\ 20\ additional\ income = \$2{,}162{,}664$

$Year\ 20\ discounted\ cash\ flow = \frac{Year\ 20\ cash\ flow}{(1 + interest\ rate)^{20\ year}} = \$321{,}466$

$Year\ 20\ cumulative\ present\ value = Year\ 19\ cumulative\ value + Year\ 20\ discounted\ cash\ flow = -\$30{,}552{,}669 = NPV$

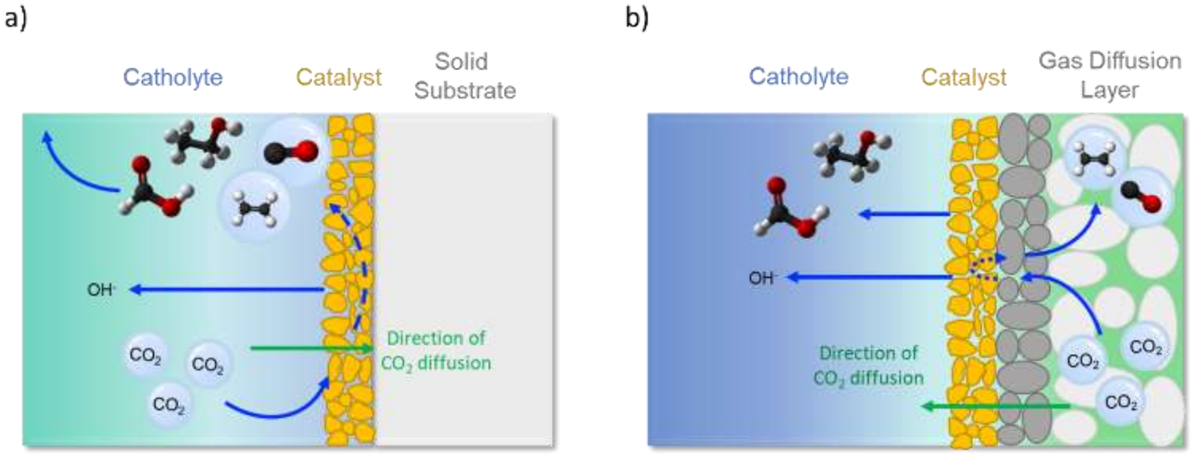

Figure S1 a) Conventional solid substrate requires CO_2 transfer from bulk electrolyte; b) gas diffusion layer enables better CO_2 transfer and product diffusion.

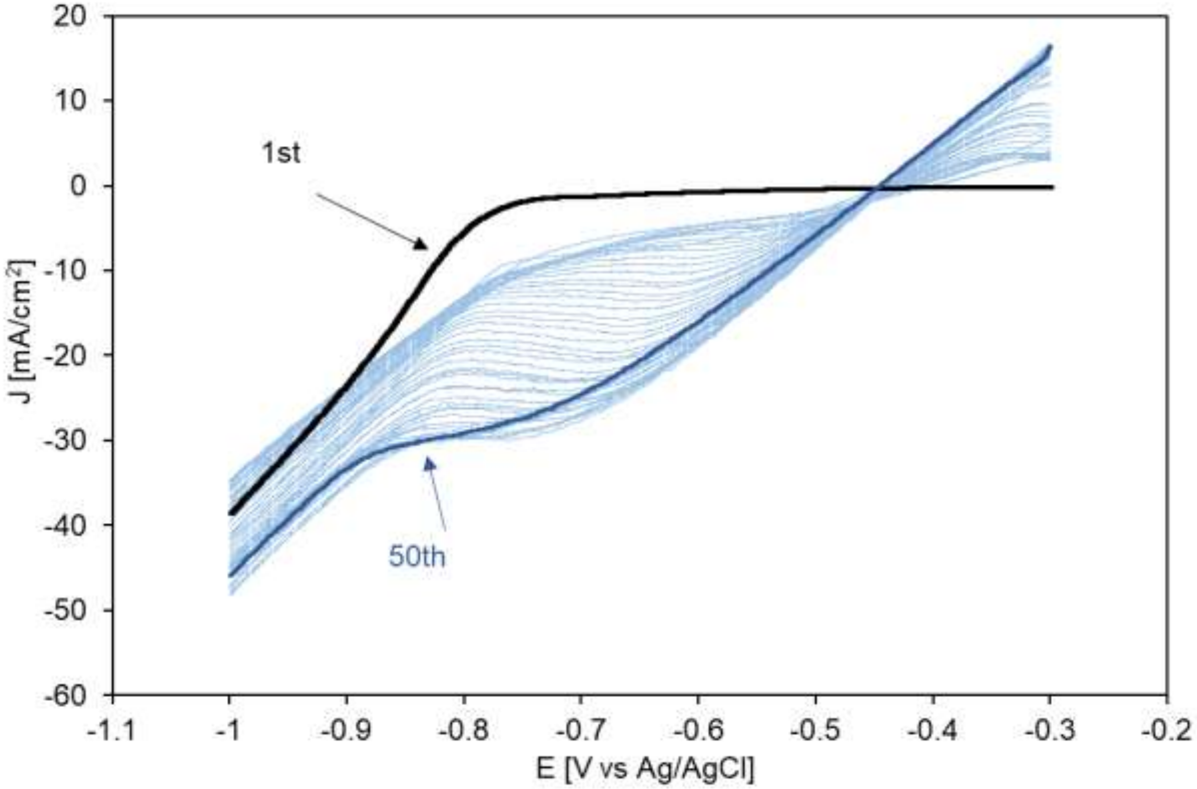

Figure S2 Potentiodynamic electrodeposition of NiP catalyst.

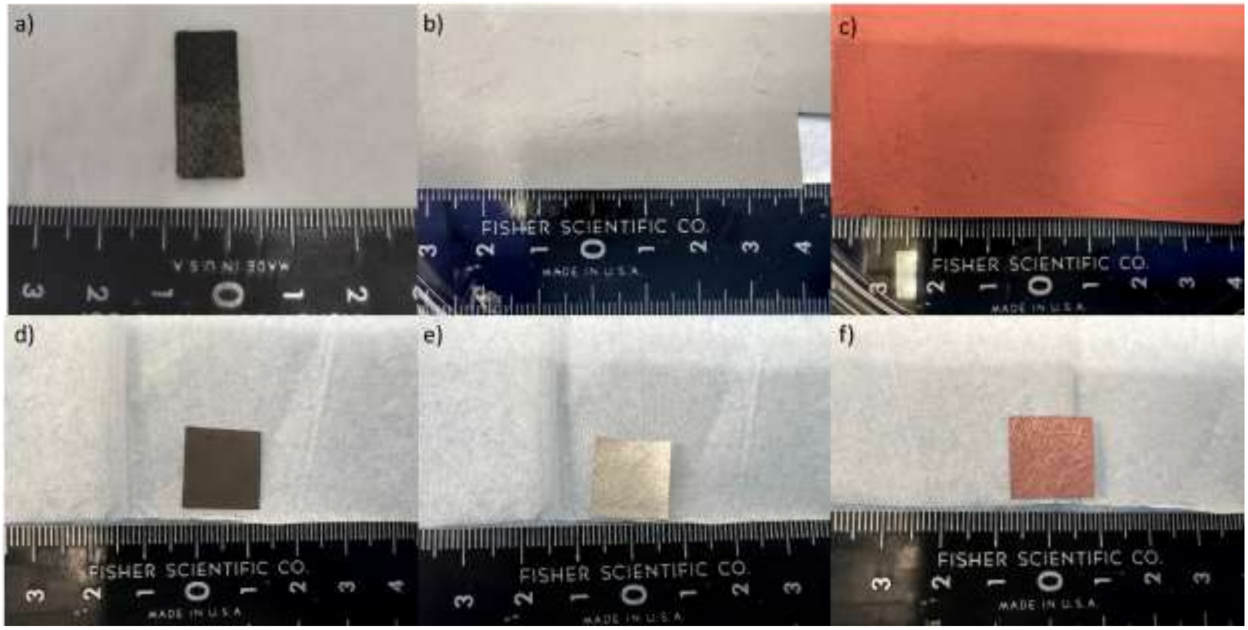

Figure S3 Photos of a) NiP@Ni/CF catalyst; b) Ag/CP catalyst; c) Cu/CP catalyst; d) Sn/CP catalyst; e) Ag/PTFE catalyst; f) Cu/PTFE catalyst.

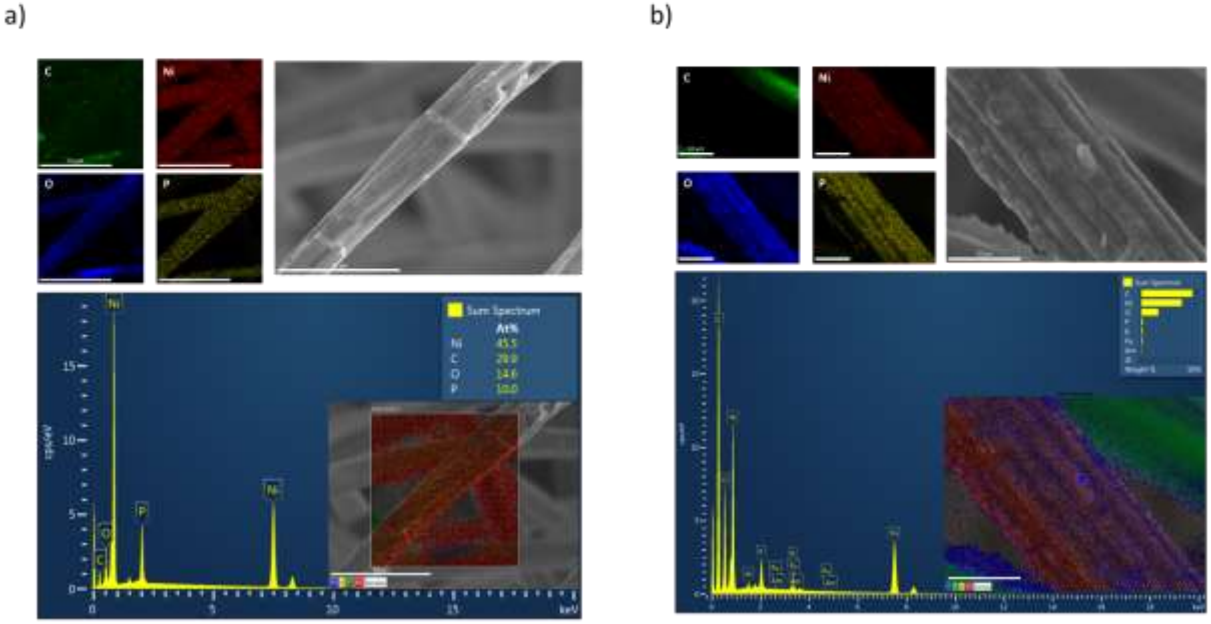

Figure S4 Energy-dispersive X-ray analysis (EDX) of a) as-prepared NiP@Ni/CF and b) post-HMFOR NiOOH/NiP@Ni/CF anode catalysts.

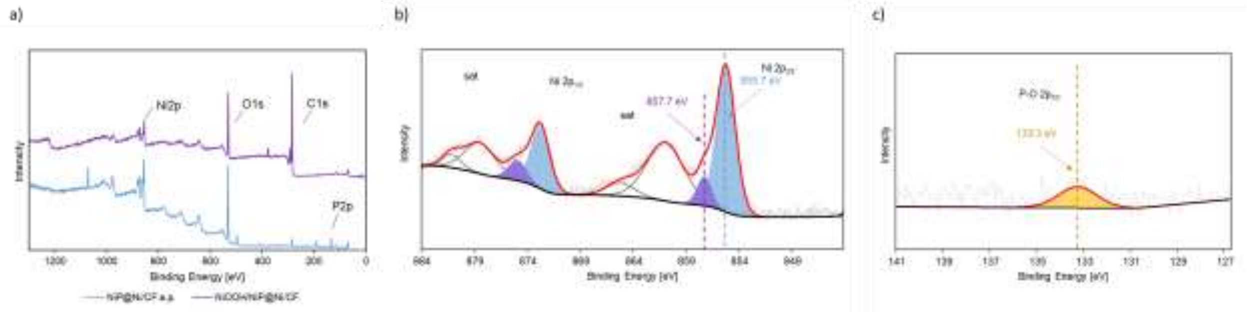

Figure S5 a) X-ray photoelectron spectroscopy (XPS) survey on as-prepared NiP@Ni/CF and post-HMFOR NiOOH/NiP@Ni/CF, and high resolution XPS on b) Ni2p and c) P2p spectra of NiOOH/NiP@Ni/CF catalyst after HMFOR.

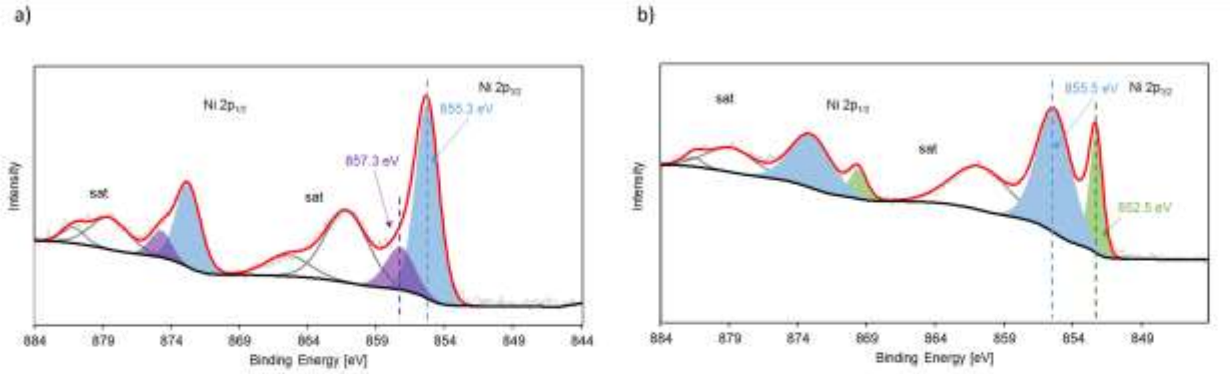

Figure S6 High resolution XPS on a) NiOOH/NF; b) Ni foam.

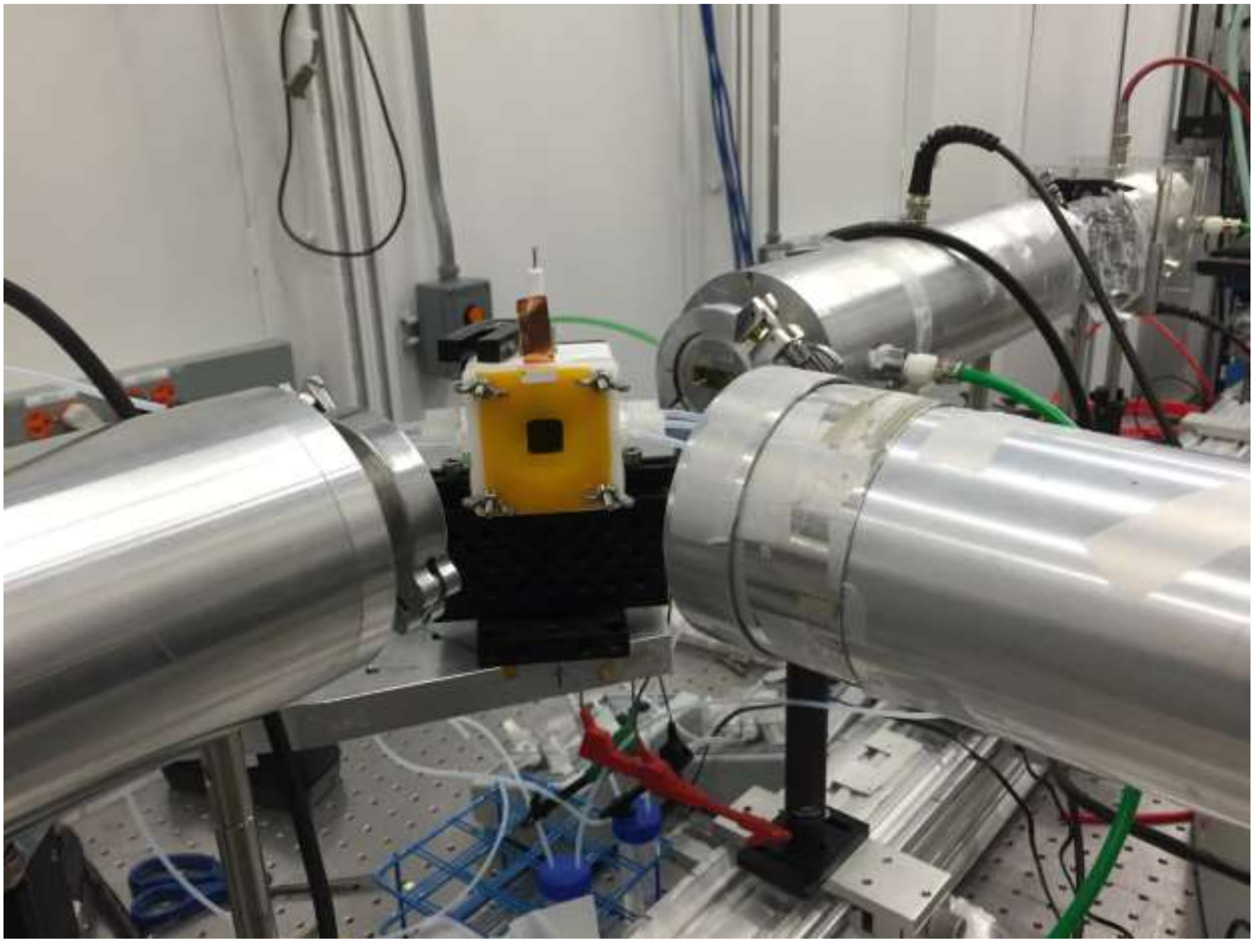

Figure S7 In-situ X-ray absorption spectroscopy (XAS) in flow cell tests at Canadian Light Source.

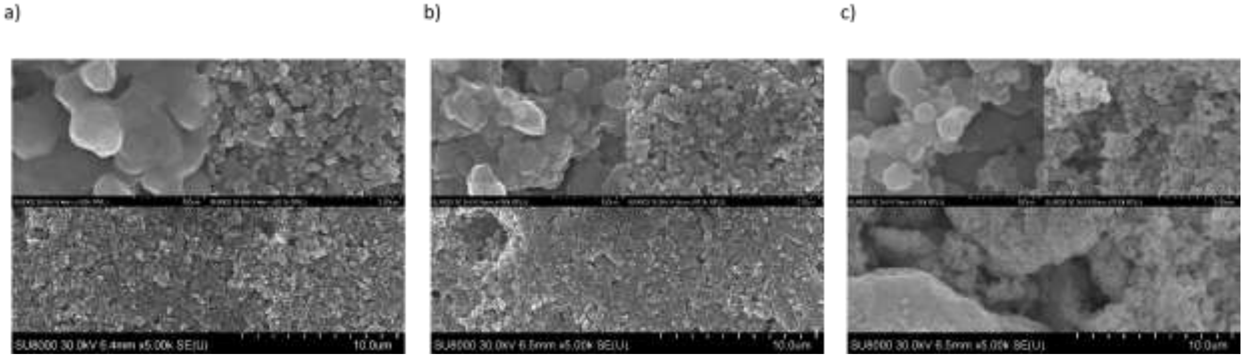

Figure S8 SEM and EDX images of a) Ag/CP, b) Cu/CP, and c) Sn/CP cathode catalysts for CO_2RR.

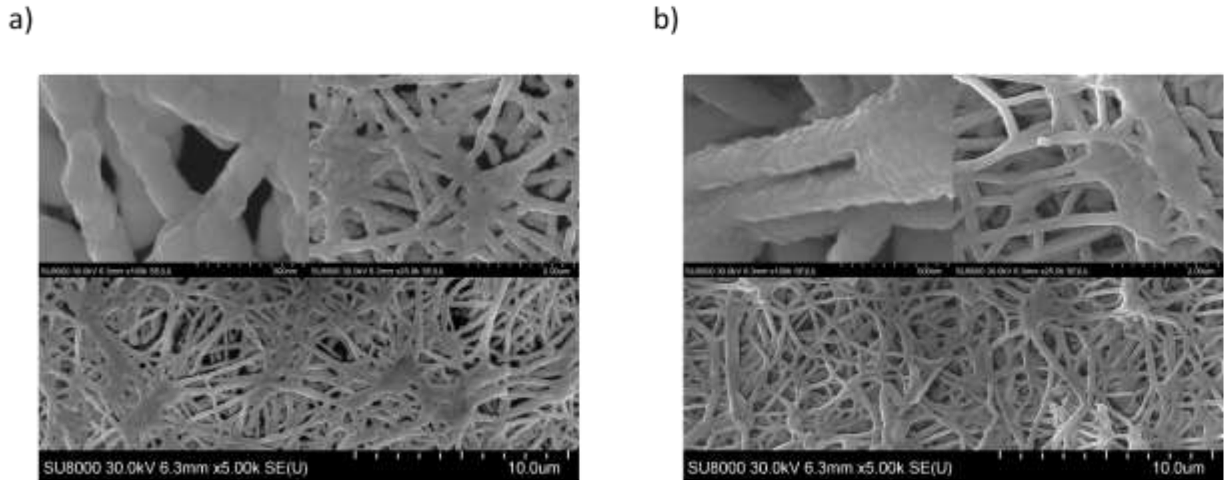

Figure S9 SEM image of a) Ag/PTFE and b) Cu/PTFE cathode catalysts for CO_2RR.

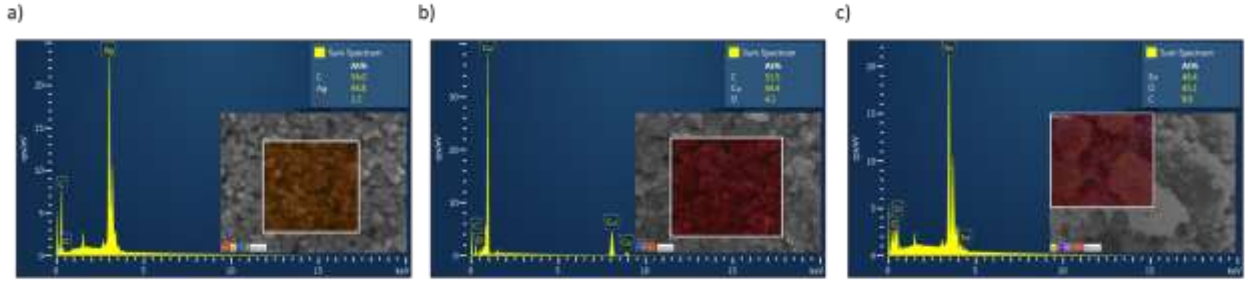

Figure S10 Energy-dispersive X-ray analysis (EDX) of Ag/CP, Cu/CP, and Sn/CP cathode catalysts.

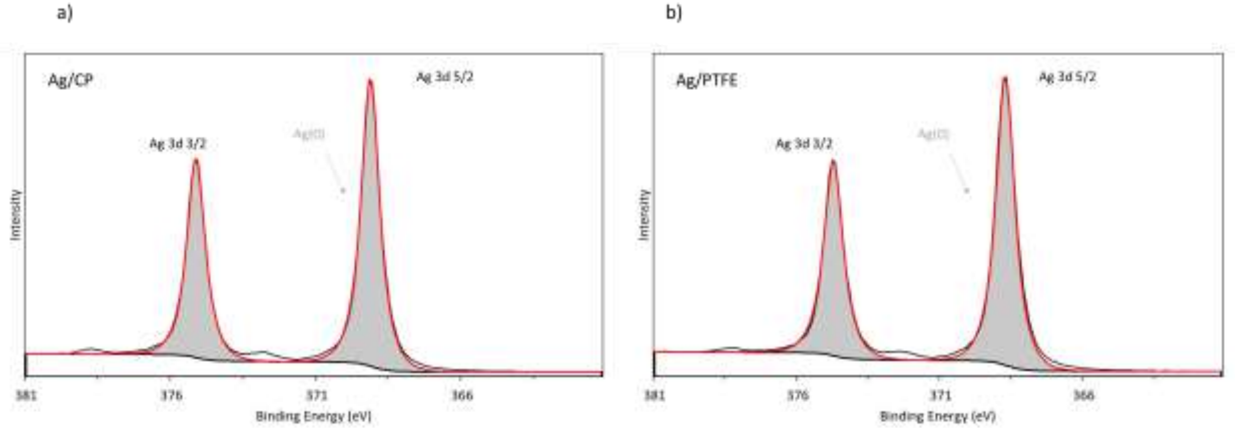

Figure S11 X-ray photoelectron spectroscopy (XPS) of a) Ag/CP and b) Ag/PTFE catalysts on Ag 3d spectra

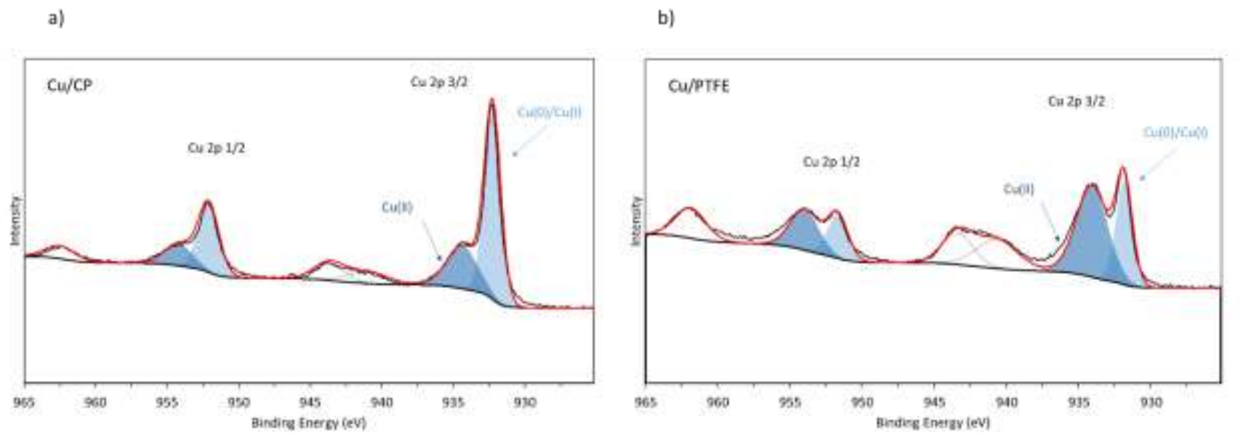

Figure S12 X-ray photoelectron spectroscopy (XPS) of a) Cu/CP and b) Cu/PTFE catalysts on Cu 2p spectra

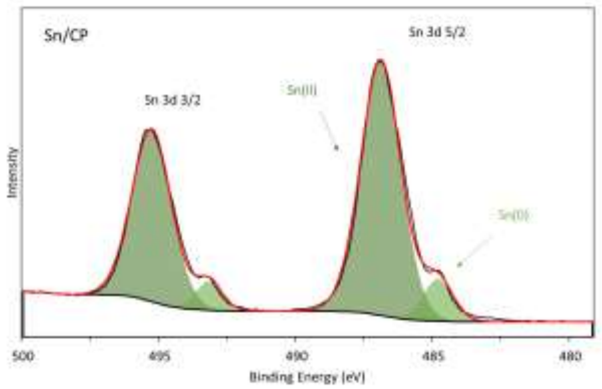

Figure S13 X-ray photoelectron spectroscopy (XPS) of Sn/CP catalysts on Sn 3d spectra

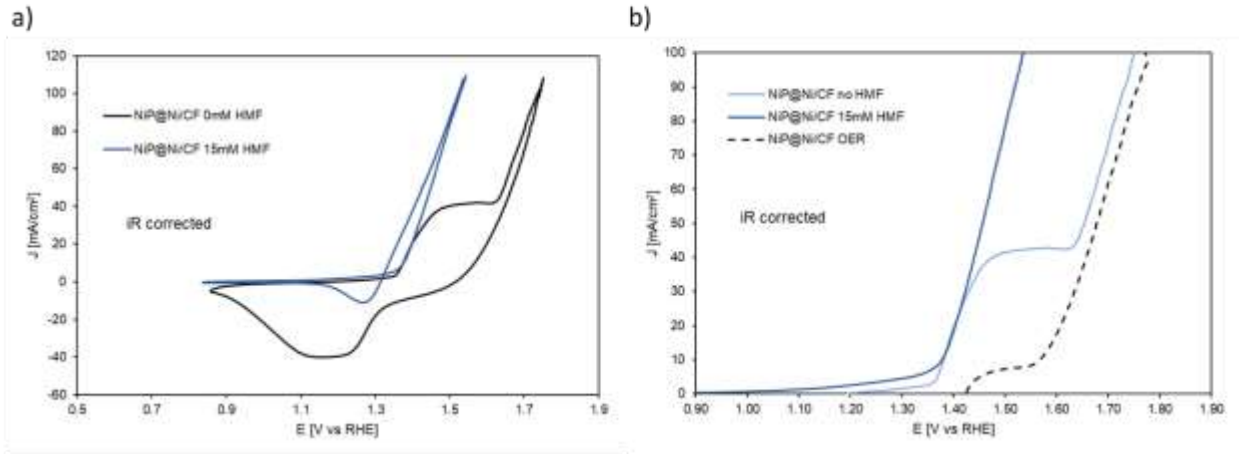

Figure S14 a) Cyclic voltammetry and b) linear sweep voltammetry of NiP catalyst in 1M KOH with and without HMF (iR corrected).

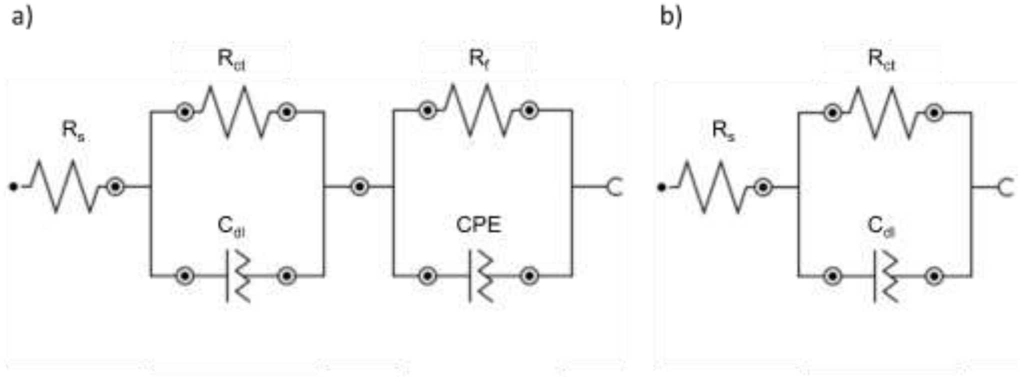

Figure S15 Electrochemical equivalent circuit for a) catalysts with inner film, and b) catalyst with thin film.

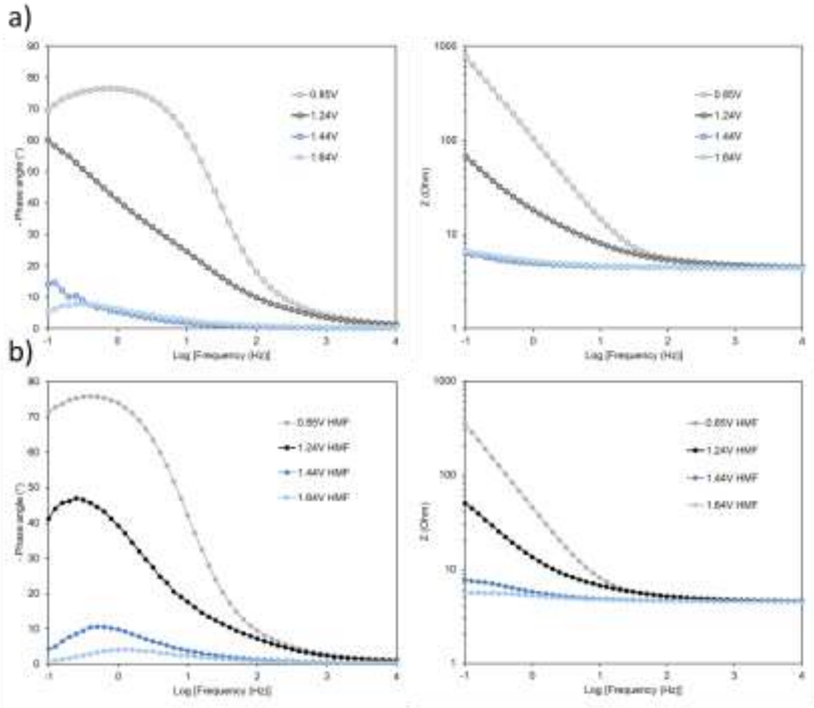

Figure S16 Bode plots of NiP a) without HMF and b) with HMF in 1M KOH.

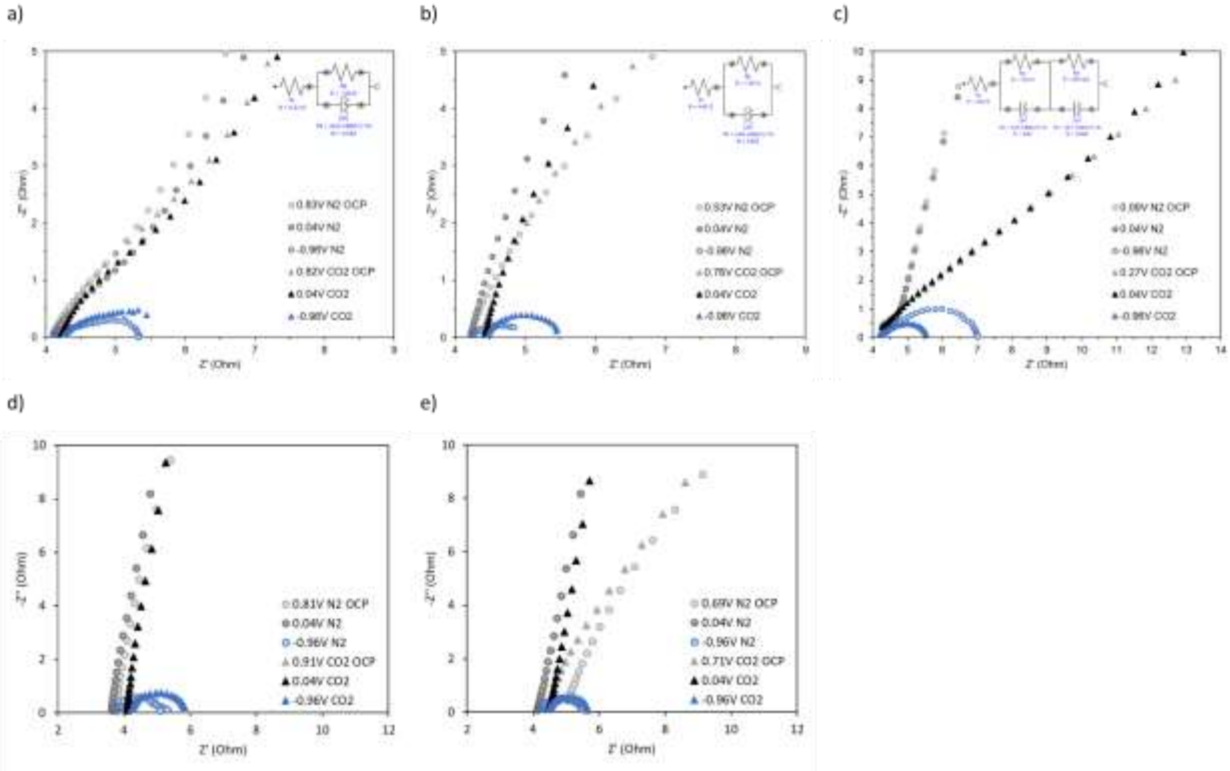

Figure S17 EIS of a) Ag/CP, b) Cu/CP, c) Sn/CP, d) Ag/PTFE, and e) Cu/PTFE cathode catalysts with and without CO_2.

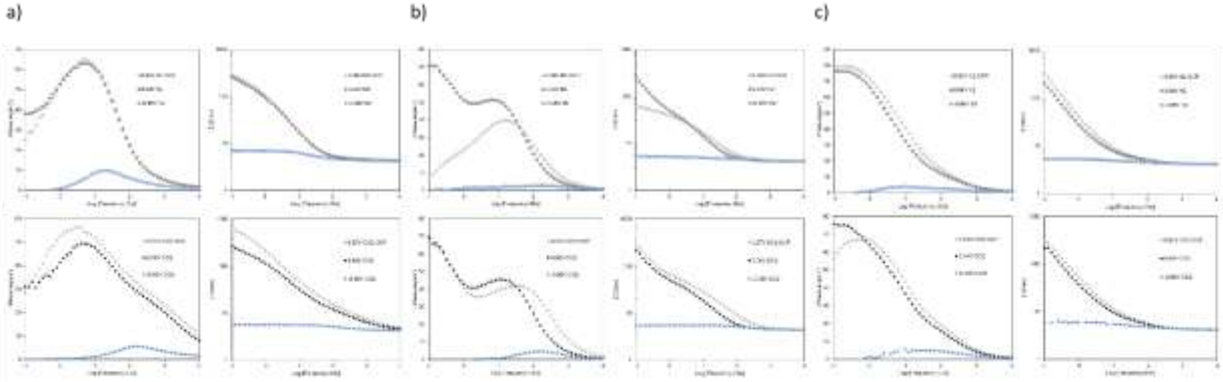

Figure S18 Bode plots of Sn/CP, Cu/CP, and Ag/CP cathode catalysts with and without CO_2.

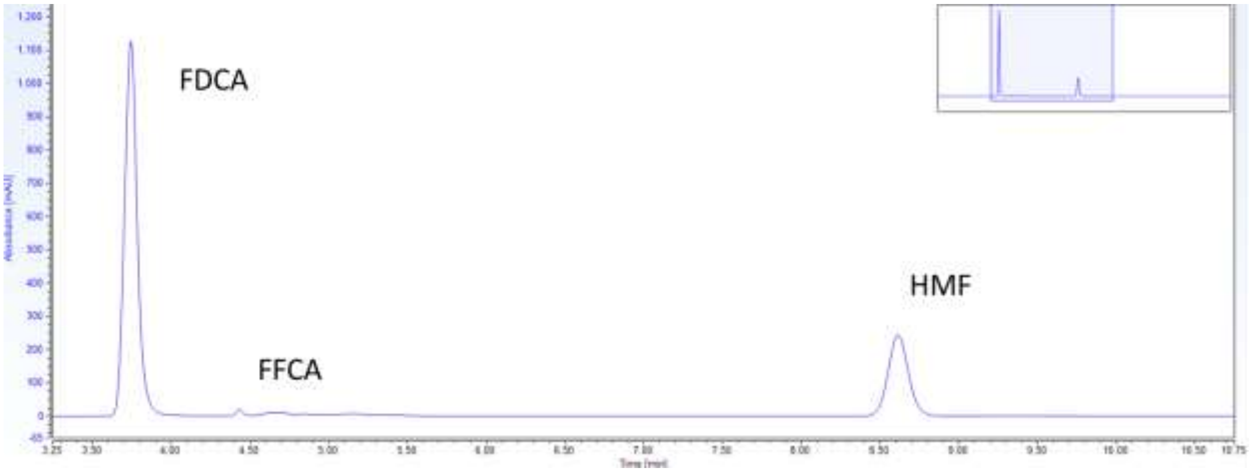

Figure S19 HPLC chromatogram on HMFOR.

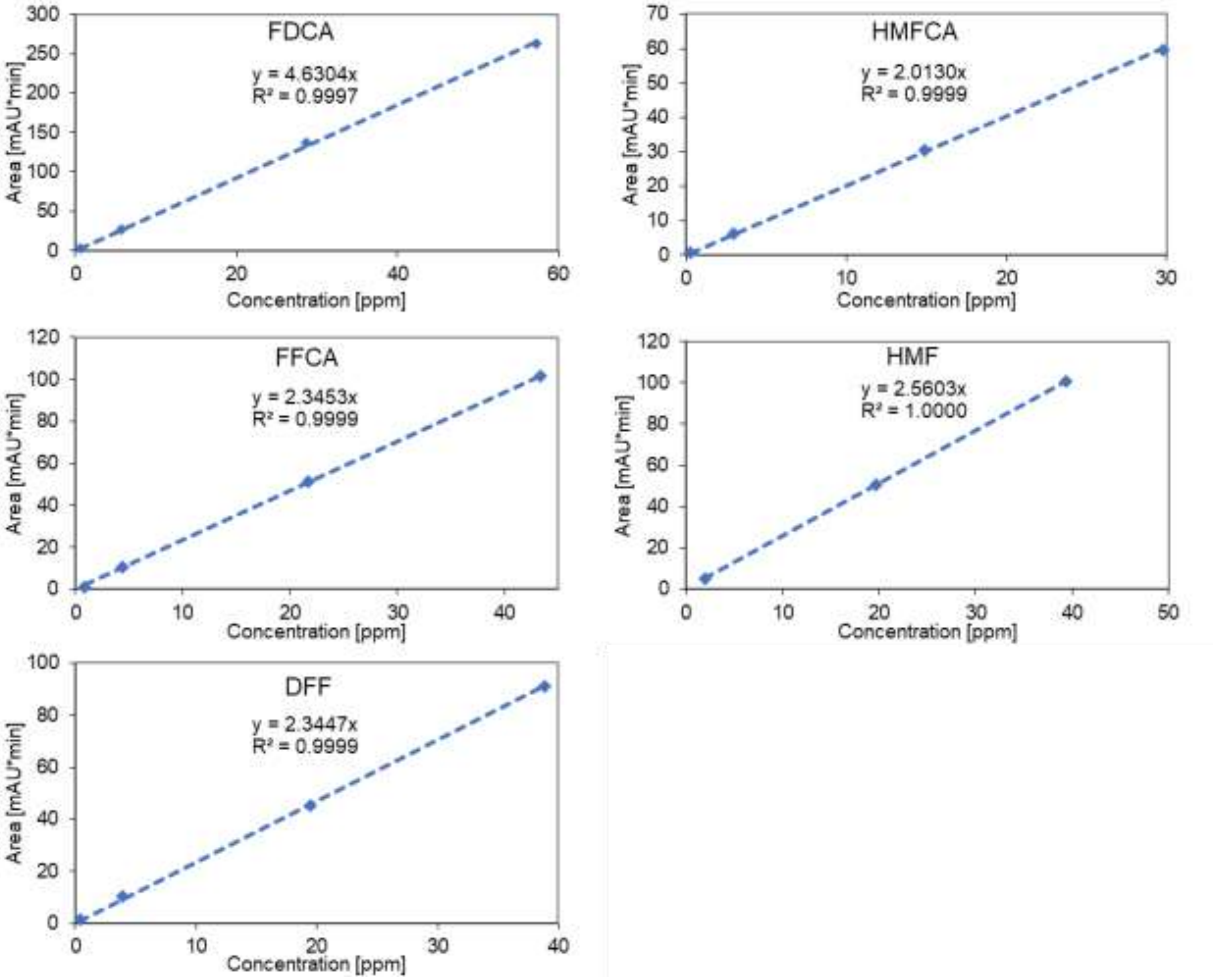

Figure S20 HPLC calibrations on HMFOR reactant, intermediates, and products.

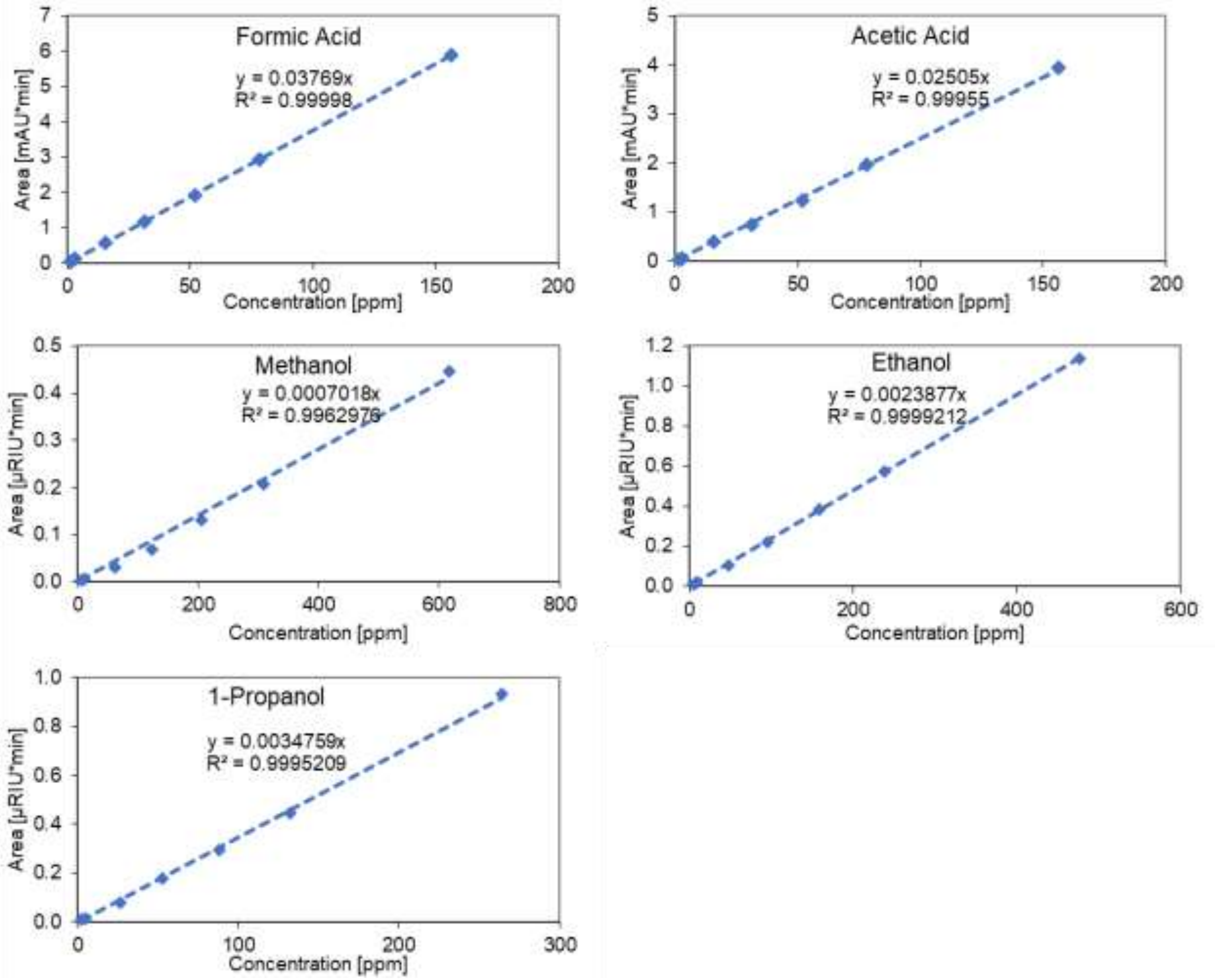

Figure S21 HPLC calibrations for CO_2RR liquid intermediates and products.

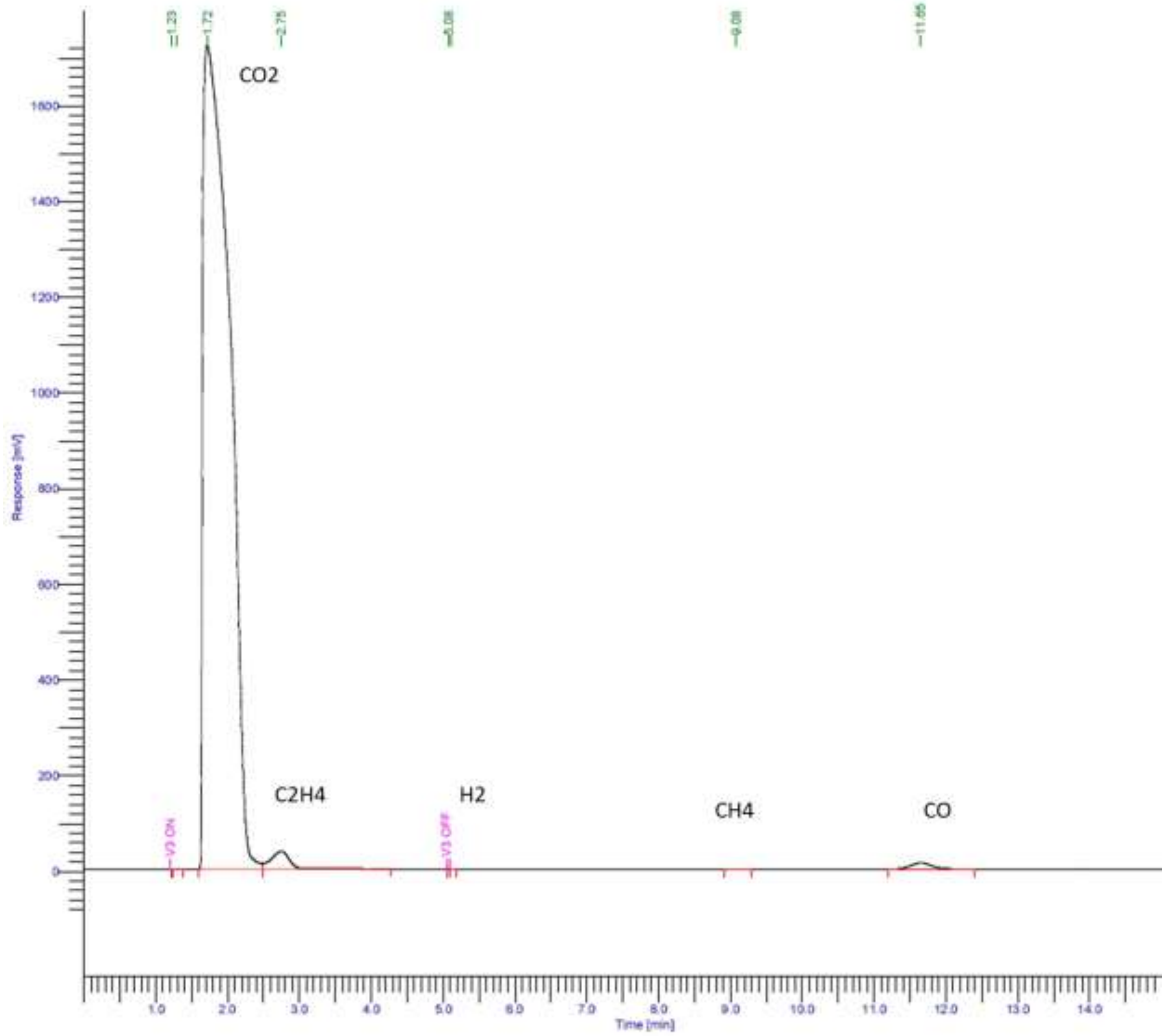

Figure S22 GC chromatogram on CO_2RR.

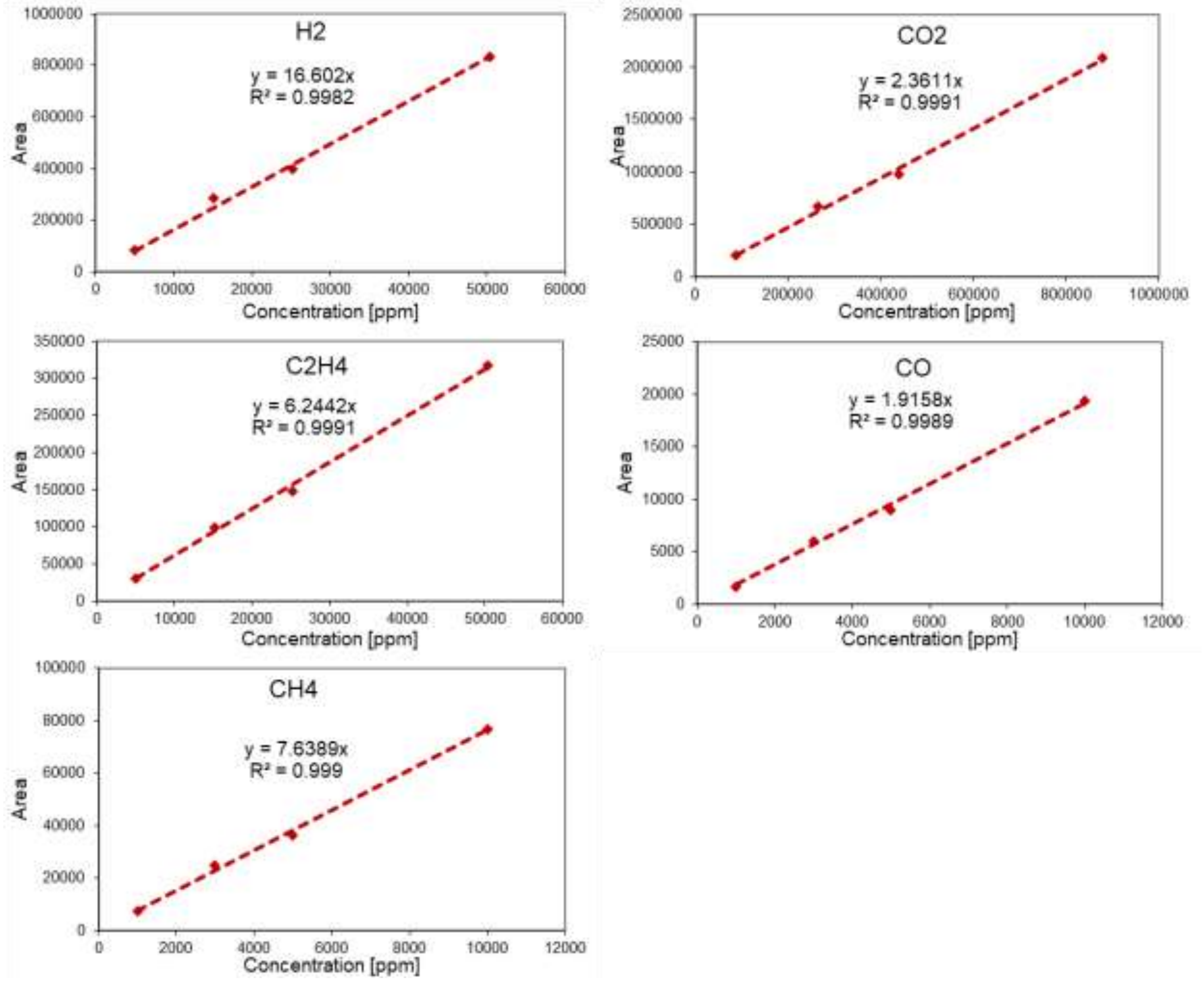

Figure S23 GC-TCD calibrations for CO_2RR gaseous intermediates and products.

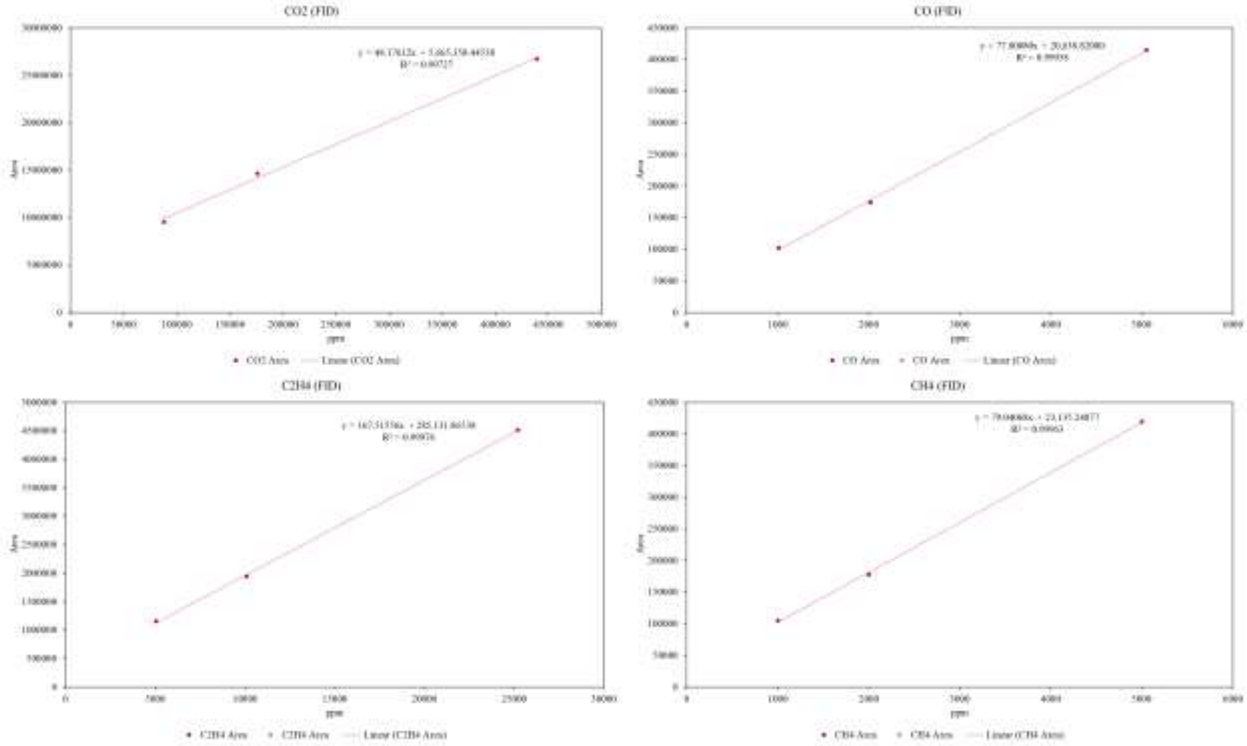

Figure S24 GC-FID calibrations for CO_2RR gaseous intermediates and products

Table S1 Linear combination fitting results including Ni foil (Ni^0) and Ni (II) oxide (Ni^{2+}) as the references.

Sample	**R-factor**	**% of Ni^0**	**% of Ni^{+2}**
NiP/CF (ex-situ)	0.00958	39.3 (± 2.0 %)	60.7
NiP/CF (in-situ @0.44 V)	0.00744	36.0 (± 1.6%)	64.0

Table S2 A comparison of the electrochemical performance of reported HMFOR electrocatalysts

Electrode Materials	**HMF [mM]**	**Electrolyte**	**Potential [V RHE]**	**Current density [mA cm^{-2}]**	**Tafel slope [mV dec^{-1}]**	**FDCA FE [%]**	**Ref.**
$NiCo_2O_4$/NF	5	1M KOH	1.53	14.83	135.7	87.5	[13]
Ni_xB/NF	10	1M KOH	1.45	100	N/A	~100	[14]
NiFe LDH	10	1M KOH	1.33	36.9	75	98.6	[15]
Ni_2P NPA/NF	10	1M KOH	1.423	> 200	N/A	98	[16]
Ni_3S_2/NF	10	1M KOH	1.423	> 200	N/A	98	[17]
NiCoFe LDH	5	1M NaOH	1.52	10	68	~90	[18]
hp-Ni	10	1M KOH	1.423	80	N/A	98	[19]
Ni_3N@C	10	1M KOH	1.38	50	48.9	99	[20]
Co-P/CF	50	1M KOH	1.38	20	N/A	~90	[21]
$Co_{0.4}NiS$@NF	10	1M KOH	1.45	100	94	99	[22]
NiCoMn-LDHs	1	1M NaOH	1.60	50	118	91.7	[23]
NiP@Ni/CF	15	1M KOH	1.38	75	35.8	85	*This work*
NiP@Ni/CF	15	1M KOH	1.42	100	35.8	78	*This work*

Table S3 CO$_2$RR-HMFOR combined system and CO$_2$RR-OER conventional system product data

Current	**Analyte**	**System**	**Cathode Products and FE**							**Anode Products and FE**			
25mA			FA	AA	EtOH	1-prOH	C_2H_4	CO	H_2	FDCA	HMFCA	FFCA	DFF
Average	no HMF	NiP//Sn/CP	61.89	0.00	0.00	0.00	0.00	21.99	10.33				
	HMF	NiP//Sn/CP HMF	60.85	0.00	0.00	0.00	0.00	15.66	5.98	61.26	13.68	12.14	2.96
	no HMF	NiP//Cu/CP	18.22	5.17	5.68	7.45	5.09	40.77	17.34				
	HMF	NiP//Cu/CP HMF	18.73	10.83	15.99	2.14	3.91	31.57	15.24	55.38	15.65	12.34	4.86
	no HMF	NiP//Ag/CP	4.94	0.00	0.00	0.00	0.00	90.10	0.29				
	HMF	NiP//Ag/CP HMF	3.51	0.00	0.00	0.00	0.00	95.02	1.24	56.40	17.82	12.69	4.06
Deviation	no HMF	NiP//Sn/CP	1.68	0.00	0.00	0.00	0.00	2.82	4.88				
	HMF	NiP//Sn/CP HMF	2.57	0.00	0.00	0.00	0.00	0.95	1.20	1.39	0.03	0.15	0.53
	no HMF	NiP//Cu/CP	1.57	1.96	1.83	2.93	8.82	2.08	0.74				
	HMF	NiP//Cu/CP HMF	1.53	0.09	1.62	0.00	0.00	1.15	1.34	1.07	1.24	0.70	0.52
	no HMF	NiP//Ag/CP	1.92	0.00	0.00	0.00	0.00	3.20	0.26				
	HMF	NiP//Ag/CP HMF	0.87	0.00	0.00	0.00	0.00	2.89	0.31	0.89	0.62	0.66	0.19
100mA													
Average	no HMF	NiP//Sn/CP	80.59	0.00	0.00	0.00	0.00	7.16	2.69				
	HMF	NiP//Sn/CP HMF	79.71	0.00	0.00	0.00	0.00	8.58	2.44	76.66	8.05	6.22	1.78
	no HMF	NiP//Cu/CP	9.11	0.87	5.23	3.00	28.25	35.27	9.80				
	HMF	NiP//Cu/CP HMF	7.66	1.67	10.17	3.18	32.86	21.66	10.38	72.17	9.66	8.34	2.19
	no HMF	NiP//Ag/CP	11.05	0.00	0.00	0.00	0.00	90.59	3.80				
	HMF	NiP//Ag/CP HMF	9.09	0.00	0.00	0.00	0.00	88.95	4.70	77.77	9.72	5.46	1.71
	no HMF	NiP//Cu/PTFE	3.45	1.50	15.19	4.19	59.56	5.81	6.49				
	HMF	NiP//Cu/PTFE HMF	3.98	1.40	15.01	4.84	54.15	8.62	6.80	74.32	9.11	7.26	2.01
	no HMF	NiP//Ag/PTFE	13.79	0.00	0.00	0.00	0.00	75.84	3.74				
	HMF	NiP//Ag/PTFE HMF	18.61	0.00	0.00	0.00	0.00	78.51	3.29	75.24	7.80	7.45	2.31

Deviation	no HMF	NiP//Sn/CP	6.82	0.00	0.00	0.00	0.00	1.49	0.04				
	HMF	NiP//Sn/CP HMF	2.28	0.00	0.00	0.00	0.00	0.96	0.50	1.70	2.36	1.03	0.42
	no HMF	NiP//Cu/CP	2.74	0.12	2.05	0.25	3.46	0.68	0.28				
	HMF	NiP//Cu/CP HMF	2.19	1.45	0.51	0.50	4.24	5.49	0.17	1.59	0.68	0.76	0.28
	no HMF	NiP//Ag/CP	0.37	0.00	0.00	0.00	0.00	2.57	0.65				
	HMF	NiP//Ag/CP HMF	2.41	0.00	0.00	0.00	0.00	9.68	3.02	1.70	0.29	0.63	0.18
	no HMF	NiP//Cu/PTFE	0.71	0.22	1.26	0.19	0.36	0.15	0.19				
	HMF	NiP//Cu/PTFE HMF	0.37	0.29	1.66	0.67	3.78	2.55	0.12	1.53	4.43	3.17	1.13
	no HMF	NiP//Ag/PTFE	1.19	0.00	0.00	0.00	0.00	6.52	2.67				
	HMF	NiP//Ag/PTFE HMF	0.68	0.00	0.00	0.00	0.00	2.74	2.14	1.83	2.96	1.78	0.94

Table S4 A comparison of the electrochemical performance of reported HMFOR electrocatalysts

Product	**Catholyte**	**J**	**FE**	**Vcat**	**Cathode Catalyst**	**Van**	**Anode Catalyst**	**Van'**	**Vcell**	**Vcell'**	**EEcell (%)**	**EEcell' (%)**	**Improv. %**	**Ref.**
CO	1M KOH	14	99	-0.6	Ag	1.63	Ni	1.41	2.2	2.0	59.3	65.9	11.15	24
CO	7M KOH	90	86	-0.8	Ag-Naf (PTFE)	2	Ni	1.44	2.8	2.2	41.0	51.4	25.26	25
CO	1M KOH	300	93	-0.65	Pd/C-PDDA		Graphite	1.87		2.5		49.3		26
Formate	0.1M KHCO3	6	80	-0.8	SnO$_2$ pNW		Pt	1.39		2.2		52.2		27
Formate	0.1M KHCO3	2	98	-0.8	Bi/rGO		Pt	1.38		2.2		66.7		28
Formate	0.4M K2SO4	500	90	-2.9	SnO2 NP	3	Ni foam	2.20	5.9	5.1	21.8	25.2	15.69	29
Methanol	[Bmim]BF4 (25 mol%)aq	67	89	-1.26	Sn/V-CuO	2.02	Pt	1.43	3.3	2.7	57.3	69.8	21.90	30
Methane	1.5M KHCO3	250	48	-0.98	sputtered Cu		Ni foam	1.78		2.8		18.5		31
Acetate	saturated NaHCO3	110	49	-1.13	Mo8@Cu/TNA		Pt net	1.44		2.6		20.9		32
Ethanol	1M KOH	160	52	-0.68	N–C/Cu	2.99	Ni foam	1.63	3.67	2.3	16.2	25.8	58.87	33
Ethylene	0.5M KCl	75	77.3	-0.9	DVL-Cu	2.2	Pt foil	1.43	3.1	2.3	28.7	38.1	32.91	34
1-Propanol	0.5 M NaHCO3	1	30	-0.41	GN/ZnO/Cu2O		Pt coil	1.37		1.8		19.2		35
1-Propanol	0.1 M KCl	6	8.7	-1.60	biphasic Cu2O		Pt plate	1.39		3.0		3.3		36

Table S5 System energy efficiencies at 100 mA/cm^2 improved by combination of anode HMFOR with ideal cathode CO$_2$RR FE and potential for each product.

Product	**Catalyst**	**Vcat (RHE)**	**Van' (RHE)**	**EE (%)**	**EE' (%)**	**Improv. (%)**
Formate	Sn/CP	-0.25	1.43	77.5	88.1	13.76
Formate	Cu/CP	-0.25	1.43	77.5	88.1	13.76
Acetate	Cu/CP	0.125	1.43	72.0	84.7	17.71
CO	Cu/CP	-0.106	1.43	75.7	87.0	15.05
Ethylene	Cu/CP	0.064	1.43	73.1	85.4	16.92
Ethanol	Cu/CP	0.084	1.43	72.7	85.2	17.17
1-Propanol	Cu/CP	0.095	1.43	72.5	85.1	17.32
CO	Ag/CP	-0.106	1.43	75.7	87.0	15.05
Formate	Cu/PTFE	-0.25	1.43	77.5	88.1	13.76
Acetate	Cu/PTFE	0.125	1.43	72.0	84.7	17.71
CO	Cu/PTFE	-0.106	1.43	75.7	87.0	15.05
Ethylene	Cu/PTFE	0.064	1.43	73.1	85.4	16.92
Ethanol	Cu/PTFE	0.084	1.43	72.7	85.2	17.17
1-Propanol	Cu/PTFE	0.095	1.43	72.5	85.1	17.32
CO	Ag/PTFE	-0.106	1.43	75.7	87.0	15.05

Table S6 System energy efficiencies at 100 mA/cm^2 improved by combination of improved anode HMFOR with observed cathode CO$_2$RR FE and potential for each product.

Product	**Catalyst**	**Vcat (RHE)**	**Van' (RHE)**	**EE (%)**	**EE' (%)**	**Improv. (%)**
Formate	Sn/CP	-0.62	1.36	52.0	59.9	15.16
Formate	Cu/CP	-0.58	1.36	5.5	6.4	15.50
Acetate	Cu/CP	-0.58	1.36	0.6	0.7	15.50
CO	Cu/CP	-0.58	1.36	17.0	19.6	15.50
Ethylene	Cu/CP	-0.58	1.36	15.9	18.4	15.50
Ethanol	Cu/CP	-0.58	1.36	3.9	4.6	15.50
1-Propanol	Cu/CP	-0.58	1.36	1.6	1.8	15.50
CO	Ag/CP	-0.69	1.36	51.1	58.6	14.67
Formate	Cu/PTFE	-0.58	1.36	2.5	2.8	15.45
Acetate	Cu/PTFE	-0.58	1.36	0.7	0.8	15.45
CO	Cu/PTFE	-0.58	1.36	4.3	5.0	15.45
Ethylene	Cu/PTFE	-0.58	1.36	29.6	34.1	15.45
Ethanol	Cu/PTFE	-0.58	1.36	7.7	8.9	15.45
1-Propanol	Cu/PTFE	-0.58	1.36	2.3	2.6	15.45
CO	Ag/PTFE	-0.76	1.36	42.6	48.7	14.16

Table S7 System energy saving factors comparison between CO_2RR-OER and CO_2RR-HMFOR with observed FE and potential.

Product	**Catalyst**	**Vcat (RHE)**	**FEcat (%)**	**Van (RHE)**	**Van’ (RHE)**	**FEan’ (%)**	**ηv’**	**ηcell’**	**Improv. (%)**
Formate	Sn/CP	-0.62	80	1.66	1.43	93	1.11	0.83	3.49
Formate	Cu/CP	-0.58	8	1.66	1.43	93	1.12	0.09	3.72
Acetate	Cu/CP	-0.58	1	1.66	1.43	93	1.12	0.01	3.72
CO	Cu/CP	-0.58	28	1.66	1.43	93	1.12	0.30	3.72
Ethylene	Cu/CP	-0.58	31	1.66	1.43	93	1.12	0.32	3.72
Ethanol	Cu/CP	-0.58	8	1.66	1.43	93	1.12	0.08	3.72
1-Propanol	Cu/CP	-0.58	3	1.66	1.43	93	1.12	0.03	3.72
CO	Ag/CP	-0.69	90	1.66	1.43	93	1.11	0.93	3.16
Formate	Cu/PTFE	-0.58	4	1.66	1.43	93	1.11	0.04	3.68
Acetate	Cu/PTFE	-0.58	1	1.66	1.43	93	1.11	0.02	3.68
CO	Cu/PTFE	-0.58	7	1.66	1.43	93	1.11	0.07	3.68
Ethylene	Cu/PTFE	-0.58	57	1.66	1.43	93	1.11	0.59	3.68
Ethanol	Cu/PTFE	-0.58	15	1.66	1.43	93	1.11	0.16	3.68
1-Propanol	Cu/PTFE	-0.58	5	1.66	1.43	93	1.11	0.05	3.68
CO	Ag/PTFE	-0.76	77	1.66	1.43	93	1.11	0.79	2.82

Table S8 System energy saving factors comparison between CO_2RR-OER and improved CO_2RR-HMFOR with ideal cathode FE and potential.

Product	**Catalyst**	**Vcat (RHE)**	**FEcat (%)**	**Van (RHE)**	**Van' (RHE)**	**FEan' (%)**	**ηv'**	**ηcell'**	**Improv. (%)**
Formate	Sn/CP	-0.25	100	1.66	1.36	100	1.19	1.19	18.63
Formate	Cu/CP	-0.25	100	1.66	1.36	100	1.19	1.19	18.63
Acetate	Cu/CP	0.125	100	1.66	1.36	100	1.24	1.24	24.29
CO	Cu/CP	-0.106	100	1.66	1.36	100	1.20	1.20	20.46
Ethylene	Cu/CP	0.064	100	1.66	1.36	100	1.23	1.23	23.15
Ethanol	Cu/CP	0.084	100	1.66	1.36	100	1.24	1.24	23.51
1-Propanol	Cu/CP	0.095	100	1.66	1.36	100	1.24	1.24	23.72
CO	Ag/CP	-0.106	100	1.66	1.36	100	1.20	1.20	20.46
Formate	Cu/PTFE	-0.25	100	1.66	1.36	100	1.19	1.19	18.63
Acetate	Cu/PTFE	0.125	100	1.66	1.36	100	1.24	1.24	24.29
CO	Cu/PTFE	-0.106	100	1.66	1.36	100	1.20	1.20	20.46
Ethylene	Cu/PTFE	0.064	100	1.66	1.36	100	1.23	1.23	23.15
Ethanol	Cu/PTFE	0.084	100	1.66	1.36	100	1.24	1.24	23.51
1-Propanol	Cu/PTFE	0.095	100	1.66	1.36	100	1.24	1.24	23.72
CO	Ag/PTFE	-0.106	100	1.66	1.36	100	1.20	1.20	21.15

References

1. D. M. Weekes, D. A. Salvatore, A. Reyes, A. Huang and C. P. Berlinguette, *Accounts of Chemical Research*, 2018, **51**, 910-918.
2. K. Liu, W. A. Smith and T. Burdyny, *ACS Energy Lett*, 2019, **4**, 639-643.
3. T. Burdyny and W. A. Smith, *Energy & Environmental Science*, 2019, **12**, 1442-1453.
4. M. G. Kibria, J. P. Edwards, C. M. Gabardo, C. T. Dinh, A. Seifitokaldani, D. Sinton and E. H. Sargent, *Adv Mater*, 2019, **31**, e1807166.
5. R. Lin, J. Guo, X. Li, P. Patel and A. Seifitokaldani, *Catalysts*, 2020, **10**.
6. L. C. Weng, A. T. Bell and A. Z. Weber, *Phys Chem Chem Phys*, 2018, **20**, 16973-16984.
7. J. Song, H. Song, B. Kim and J. Oh, *Catalysts*, 2019, **9**.
8. R. Lin, M. Salehi, J. Guo and A. Seifitokaldani, *iScience*, 2022, **25**, 104744.
9. M. S. Rafique, M. Rafique, M. B. Tahir, S. Hajra, T. Nawaz and F. Shafiq, in *Nanotechnology and Photocatalysis for Environmental Applications*, eds. M. B. Tahir, M. Rafique and M. S. Rafique, Elsevier, 2020, DOI: https://doi.org/10.1016/B978-0-12-821192-2.00003-6, pp. 45-56.
10. H. Schultz, G. Bauer, E. Schachl, F. Hagedorn and P. Schmittinger, in *Ullmann's Encyclopedia of Industrial Chemistry*, 2000, DOI: https://doi.org/10.1002/14356007.a22_039.
11. W. M. Haynes, *CRC Handbook of Chemistry and Physics, 95th Edition*, CRC Press Hoboken, Hoboken, 95th ed edn., 2014.
12. A. Frontier, Magic Formulas for Aqueous Solutions (Basic), http://www.chem.rochester.edu/notvoodoo/pages/magic_formulas.php?page=basic, 2023).
13. M. J. Kang, H. Park, J. Jegal, S. Y. Hwang, Y. S. Kang and H. G. Cha, *Applied Catalysis B: Environmental*, 2019, **242**, 85-91.
14. S. Barwe, J. Weidner, S. Cychy, D. M. Morales, S. Dieckhöfer, D. Hiltrop, J. Masa, M. Muhler and W. Schuhmann, *Angewandte Chemie International Edition*, 2018, **57**, 11460-11464.
15. W.-J. Liu, L. Dang, Z. Xu, H.-Q. Yu, S. Jin and G. W. Huber, *ACS Catalysis*, 2018, **8**, 5533-5541.
16. B. You, N. Jiang, X. Liu and Y. Sun, *Angewandte Chemie International Edition*, 2016, **55**, 9913-9917.
17. B. You, X. Liu, N. Jiang and Y. Sun, *Journal of the American Chemical Society*, 2016, **138**, 13639-13646.
18. M. Zhang, Y. Liu, B. Liu, Z. Chen, H. Xu and K. Yan, *ACS Catalysis*, 2020, **10**, 5179-5189.
19. B. You, X. Liu, X. Liu and Y. Sun, *ACS Catalysis*, 2017, **7**, 4564-4570.
20. N. Zhang, Y. Zou, L. Tao, W. Chen, L. Zhou, Z. Liu, B. Zhou, G. Huang, H. Lin and S. Wang, *Angewandte Chemie International Edition*, 2019, **58**, 15895-15903.
21. N. Jiang, B. You, R. Boonstra, I. M. Terrero Rodriguez and Y. Sun, *ACS Energy Letters*, 2016, **1**, 386-390.
22. Y. Sun, J. Wang, Y. Qi, W. Li and C. Wang, *Adv Sci (Weinh)*, 2022, **9**, e2200957.
23. B. Liu, S. Xu, M. Zhang, X. Li, D. Decarolis, Y. Liu, Y. Wang, E. K. Gibson, C. R. A. Catlow and K. Yan, *Green Chemistry*, 2021, **23**, 4034-4043.
24. W.-H. Cheng, M. H. Richter, I. Sullivan, D. M. Larson, C. Xiang, B. S. Brunschwig and H. A. Atwater, *ACS Energy Letters*, 2020, **5**, 470-476.
25. C. M. Gabardo, A. Seifitokaldani, J. P. Edwards, C.-T. Dinh, T. Burdyny, M. G. Kibria, C. P. O'Brien, E. H. Sargent and D. Sinton, *Energy & Environmental Science*, 2018, **11**, 2531-2539.
26. R. Xia, S. Zhang, X. Ma and F. Jiao, *Journal of Materials Chemistry A*, 2020, **8**, 15884-15890.
27. B. Kumar, V. Atla, J. P. Brian, S. Kumari, T. Q. Nguyen, M. Sunkara and J. M. Spurgeon, *Angew Chem Int Ed Engl*, 2017, **56**, 3645-3649.
28. Y. X. Duan, K. H. Liu, Q. Zhang, J. M. Yan and Q. Jiang, *Small Methods*, 2020, **4**.

29. Y. Chen, A. Vise, W. E. Klein, F. C. Cetinbas, D. J. Myers, W. A. Smith, T. G. Deutsch and K. C. Neyerlin, *ACS Energy Letters*, 2020, **5**, 1825-1833.
30. W. Guo, S. Liu, X. Tan, R. Wu, X. Yan, C. Chen, Q. Zhu, L. Zheng, J. Ma, J. Zhang, Y. Huang, X. Sun and B. Han, *Angew Chem Int Ed Engl*, 2021, **60**, 21979-21987.
31. A. Sedighian Rasouli, X. Wang, J. Wicks, G. Lee, T. Peng, F. Li, C. McCallum, C.-T. Dinh, A. H. Ip, D. Sinton and E. H. Sargent, *ACS Sustainable Chemistry & Engineering*, 2020, **8**, 14668-14673.
32. D. Zang, Q. Li, G. Dai, M. Zeng, Y. Huang and Y. Wei, *Applied Catalysis B: Environmental*, 2021, **281**.
33. X. Wang, Z. Wang, F. P. García de Arquer, C.-T. Dinh, A. Ozden, Y. C. Li, D.-H. Nam, J. Li, Y.-S. Liu, J. Wicks, Z. Chen, M. Chi, B. Chen, Y. Wang, J. Tam, J. Y. Howe, A. Proppe, P. Todorović, F. Li, T.-T. Zhuang, C. M. Gabardo, A. R. Kirmani, C. McCallum, S.-F. Hung, Y. Lum, M. Luo, Y. Min, A. Xu, C. P. O’Brien, B. Stephen, B. Sun, A. H. Ip, L. J. Richter, S. O. Kelley, D. Sinton and E. H. Sargent, *Nature Energy*, 2020, **5**, 478-486.
34. W. Liu, P. Zhai, A. Li, B. Wei, K. Si, Y. Wei, X. Wang, G. Zhu, Q. Chen, X. Gu, R. Zhang, W. Zhou and Y. Gong, *Nat Commun*, 2022, **13**, 1877.
35. R. A. Geioushy, M. M. Khaled, K. Alhooshani, A. S. Hakeem and A. Rinaldi, *Electrochimica Acta*, 2017, **245**, 456-462.
36. S. Lee, D. Kim and J. Lee, *Angew Chem Int Ed Engl*, 2015, **54**, 14701-14705.